NASA CR 54821
AGC 8800-58

# THE MECHANICAL DESIGN OF A TWO-STAGE IMPULSE TURBINE FOR THE LIQUID HYDROGEN TURBOPUMP OF THE M-1 ENGINE

By

T. W. Reynolds



Prepared for

National Aeronautics and Space Administration

Contract NAS 3-2555

AEROJET GENERAL TIRE GENERAL

AEROJET-GENERAL CORPORATION

SACRAMENTO, CALIFORNIA

NASA CR 54821
AGC 8800-58

TECHNOLOGY REPORT

# THE MECHANICAL DESIGN OF A TWO-STAGE IMPULSE TURBINE FOR THE LIQUID HYDROGEN TURBOPUMP OF THE M-1 ENGINE

Prepared for

NATIONAL AERONAUTICS AND SPACE ADMINISTRATION

30 May 1966

CONTRACT NAS 3-2555

Prepared by:

AEROJET-GENERAL CORPORATION
LIQUID ROCKET OPERATIONS
SACRAMENTO, CALIFORNIA

AUTHOR: T. W. Reynolds

APPROVED: W. E. Watters
Manager
M-1 Turbopump Project

Technical Management:

NASA LEWIS RESEARCH CENTER
CLEVELAND, OHIO

TECHNICAL MANAGER: D. D. Scheer

APPROVED: W. W. Wilcox
M-1 Project Manager

## ABSTRACT



This report describes the mechanical and structural design of the two-row Curtis turbine for the hydrogen turbopump of the M-1 Engine. The turbine is a lightweight direct drive unit with a design point power output of 88,150 hp at 13,225 rpm, and a thermal efficiency of 62.8%. Operating temperature gradients from -420°F to +1200°F are accommodated by fabricating the housings from thin, welded shells of Inconel 718 alloy and supporting the housings near the axial center point of the blade rows by an external frame.

TABLE OF CONTENTS

TABLE OF CONTENTS (Cont'd)

## TABLE OF CONTENTS (Cont'd)

## LIST OF TABLES



## LIST OF FIGURES

## LIST OF FIGURES (Cont'd)

## I. SUMMARY

The turbine is designed as a flightweight, direct-drive for the M-1 liquid hydrogen pump. It is a full admission, two-row Curtis turbine, which is the type that is used extensively in high pressure steam turbines and large rocket engine turbopumps.

The aerodynamic design point power output is 88,150 hp at 13,225 rpm. The driving gas has a temperature of 1460°R and a pressure of 1000 psia. This driving gas is obtained from the combustion products of hydrogen and oxygen.

The turbine components are fabricated almost entirely of Inconel 718, a nickel-chromium alloy. This material possesses many desirable qualities, such as high strength at both cryogenic and elevated temperatures, high ductility, good stress rupture qualities, and good weldability using the gas tungsten arc weld or the electron-beam methods.

Thermal gradients are severe because the turbine soaks at liquid hydrogen temperature (-423°F) and is then shocked with hot gas at 1000°F to 1300°F. The turbine static components are all supported from a main flange by a space frame to permit unrestrained thermal movement and is free to move radially at the turbine end, while it is firmly anchored to the hydrogen pump discharge housing. The arrangement permits the housings to move freely with the thermal gradients, with only a minor affect upon blade row alignment and clearances. A flexible, bellows-type seal is provided between the floating housings and the fixed turbine rotor bearing housing.

The static components were designed with a safety factor of 1.2 upon the 0.2% yield strength, or a safety factor of 1.6 upon the ultimate strength, whichever is lower at the local temperature. The turbine blades were designed with a safety factor of 1.25 at 110% of operating speed. Stress limits were determined by plotting combined stresses on a modified Goodman diagram. The diagram failure line was used as a limit. The average effective stress in the rotor discs was limited by a 1.5 safety factor upon the ultimate strength. The rotor bore stress was limited to less than twice the yield strength at the local temperature.

This turbine offers good performance, light weight, and simple mechanical construction. The total turbine weight, including the support frame and the inlet-adapter-elbow, is 960 lb.

## II. INTRODUCTION

The turbine specified for the M-1 liquid hydrogen turbopump is a direct-drive, full admission, two-row Curtis-type (velocity staged) machine. This turbine has not been tested at full scale under hot conditions. However, a single stage turbine with some components identical to the two-row machine was tested driving

the hydrogen pump[1] to approximately 90% of design speed. The single stage turbine test results are being reported separately[2].

The pumping system for the liquid propellants of the M-1 engine consists of two separate turbopumps. The turbines are driven with gas-generator-supplied hot gas obtained from the combustion products of the liquid hydrogen and the liquid oxygen. The turbines are arranged in series, with the gas initially expanded in the liquid hydrogen turbopump turbine and then, further expanded in the liquid oxygen turbopump turbine. The exhaust gas from the liquid oxygen turbopump turbine is routed through three heat exchangers; one to heat hydrogen for the gimbal actuators, one to heat hydrogen for tank pressurization, and the other to heat oxygen for tank pressurization. The exhaust gas is then directed to the lower skirt of the engine thrust chamber for cooling the walls. Finally, the gas is ejected through a set of small nozzles to provide thrust augmentation with an approximate specific impulse of 260 lbf-sec/lbm. Figure No. 1 shows the M-1 engine turbopump and gas ducting arrangement.

The turbine components are fabricated almost entirely of Inconel 718, which is an age-hardenable nickel-chromium alloy. This material was selected because it is very ductile, it can be easily welded by the gas tungsten arc weld or the electron-beam methods, and it has high strength at both cryogenic and elevated temperature (-420°F to +1300°F).

The design, development, and fabrication of this turbine were conducted by the Aerojet-General Corporation under contract with the National Aeronautics and Space Administration. The aerodynamic design of the turbine is being reported separately[3].

## III. TECHNICAL DISCUSSION

### A. DESIGN REQUIREMENTS

#### 1. Performance

The turbine stator and rotor gas passages were designed to meet the following aerodynamic criteria:

| | |
|---|---|
| Inlet Gas Total Temperature | 1460°F |

---

(1) Regan, P. J., Mechanical Design of the M-1 Axial Flow Liquid Hydrogen Fuel Pump, NASA CR-54823, 15 February 1966

(2) Blakis, R., Lindley, B. K., Ritter, J. A., and Watters, W. E., Initial Test Evaluation of the M-1 Liquid Hydrogen Turbopump, Including Installation Test Procedures and Test Results, NASA CR-54827, 20 July 1966

(3) Reynolds, T. W., Aerodynamic Design and Estimated Performance of a Two-Stage Turbine for the M-1 Fuel Turbopump, NASA CR-54820, 15 April 1966

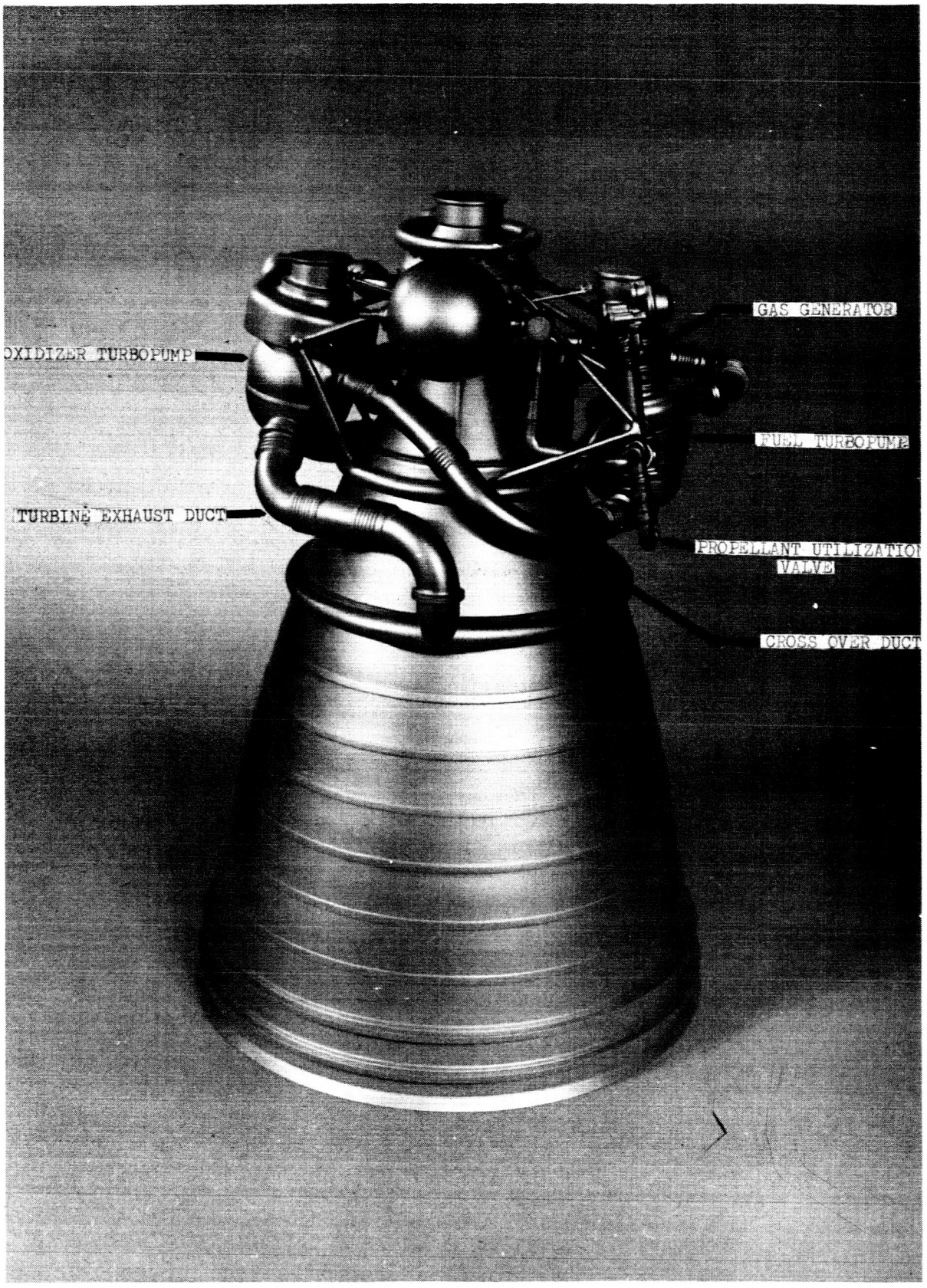


Figure 1

M-1 Engine Mockup

| | |
|---|---|
| Inlet Gas Total Pressure | 1000 psia |
| Exit Gas Total Temperature | 1134°R |
| Exit Gas Static Pressure | 214 psia |
| Shaft Speed | 13,225 rpm |
| Shaft Power | 88,150 hp |
| Shaft Torque | 35,800 ft lb |
| Gas Flow Rate | 99.3 lb/sec |
| Blade/Jet Speed Ratio ($U/C_o$) | 0.188 |
| Pressure Ratio (Inlet Total to Exit Static) | 4.673 |
| Turbine Bucket Pitch Line Diameter | 23.0-in. |
| Efficiency (Inlet Total to Exit Static) | 0.628 |

The turbine parts were designed to meet the following mechanical design criteria:

| | |
|---|---|
| Gas Inlet Total Temperature | *1300°F (1760°R) |
| Gas Inlet Total Pressure | *1175 psia |
| Gas Exit Total Temperature | 1000°F (1460°R) |
| Gas Exit Static Pressure | 386 psia |
| Shaft Power | 119,725 hp |
| Shaft Speed | 14,550 rpm |
| Shaft Torque | 43,200 ft lb |
| Run Duration | 400 sec |
| Usable Life | 10,500 sec |
| Start Cycles | 21 |
| Starting Acceleration | 0-13,225 rpm, 1.9 sec |

c. The turbine rotors to be close-coupled to the turbine bearing to achieve shaft critical speed requirements.

d. The turbine rotor weight to be minimized to achieve both shaft critical speed requirements and rotating part inertia requirements for engine starting.

e. The flightweight turbine weight goal is to be achieved.

## B. SELECTED CONFIGURATION

### 1. Description

The selected configuration is shown in Figure No. 2. It consists of a two-stage, velocity-compounded (Curtis-type) turbine set with a toroidal inlet manifold; a segmented conical support structure; a conical exhaust housing (turbopump test unit, engine turbopump design has a bifurcated hemispherical, exhaust housing); and unique, seal-welded separable turbine housing joints.

The first-stage turbine rotor is an integral unit consisting of a shaft, turbine disc, and 80 blades (see Figures No. 3 through No. 5). The shaft connects the turbine to the fuel pump rotor. Piloting diameters and a spline are provided for alignment and power transmission. The turbine shaft also carries the turbine end bearing spacers and the other rotating components needed to permit the functioning of a shaft riding seal and a lift-off seal. These latter components are parts of the power transmission assembly.

The turbine blades are shrouded to provide better performance. The shroud is split between alternate blades for minimum thermal stress and satisfactory control of blade vibration. The blades are hollow for minimum weight and stress.

The turbine disc is of minimum cross-section to reduce weight. The disc has a curvic coupling at the center on the side opposite from the shaft. This coupling is the interface for the second-stage turbine.

The second-stage rotor is an integral unit consisting of a disc and 78 blades, which have a tip shroud. This shroud is split between each blade, which is hollow for minimum weight. The turbine disc is also designed for minimum weight. A curvic coupling is provided as an interface to the first-stage turbine. Figures No. 6 through No. 8 show the rotor and blades.

A turbine tie-bolt fastens the turbine assembly to the pump rotor. This tie-bolt, which is threaded into the pump rotor at one end, has a nut and lock washer retaining system that bears against the second-stage turbine.

The turbine housings, including the inlet manifold, are mounted

Component Temperature at Start -420°F

(* The original mechanical design requirements were 1250 psia inlet total pressure and 1350°F inlet total temperature. The lower design values presented were determined to be compatible with the engine requirements and permitted the use of Inconel 718 forgings which were specified to be solution-annealed at 1950°F and aged at 1200°F to 1350°F. An 1800°F solution anneal is required to obtain adequate stress rupture properties for the higher design values originally specified.)

2. Interfaces

a. Internal Turbopump Interfaces

The turbine shaft has a spline and two piloting diameters, which form the interface with the pump rotor. The turbine shaft also carries the journals for the turbine-end roller bearing and the shaft riding seal as well as the mating face for the shaft seal. To achieve predictable and acceptable turbopump critical speeds, an interference fit between the pump rotor and the turbine shaft was specified for all operating conditions.

b. External Interfaces

The following gas duct interfaces were specified with the interface location shown in Figure No. 1.

(1) A single 8-in. inner diameter inlet for turbine drive gas.

(2) A single 5-in. inner diameter inlet for turbine bypass gas for engine calibration and propellant utilization control.

(3) Dual 11.4-in. inner diameter outlets for turbine exhaust gas.

3. Primary Mechanical Design Objectives

a. The static and rotating parts to be designed to withstand severe thermal gradients. The thermal gradients received prime consideration because the turbine is exposed to the effects of very long pump chilldowns to liquid hydrogen temperature followed by rapid startup with 1300°F hot gas. This causes the hot gas flow path to have very large transient temperatures. Some parts, such as the bearing housing and the rotor hub, are adjacent to liquid hydrogen which causes a large thermal gradient throughout the entire operating cycle.

b. Adequate static-to-rotating part clearance to be provided under all operating conditions while maintaining reasonable close tolerances to minimize leakage effects.

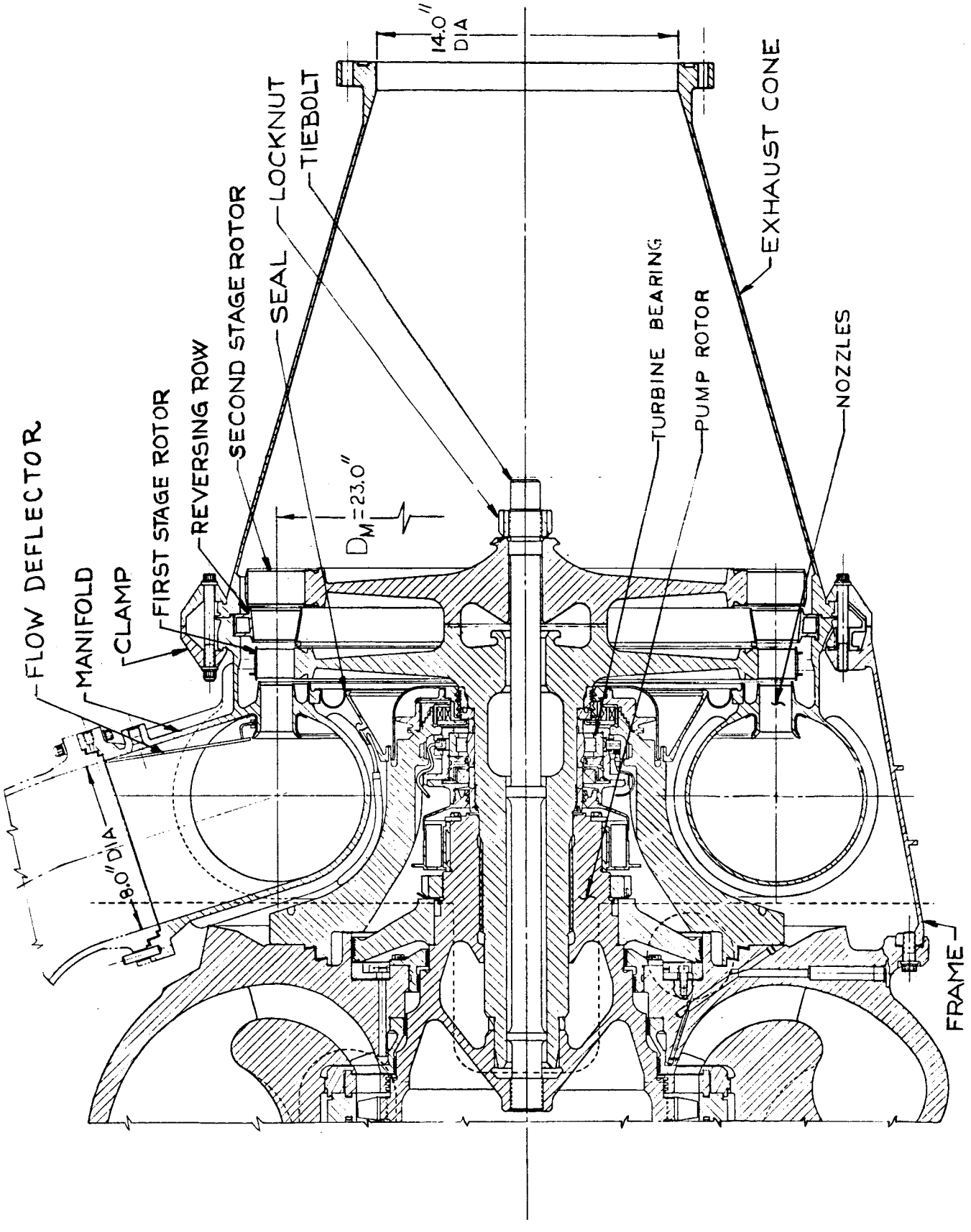


Figure 2

Turbine Components as Assembled

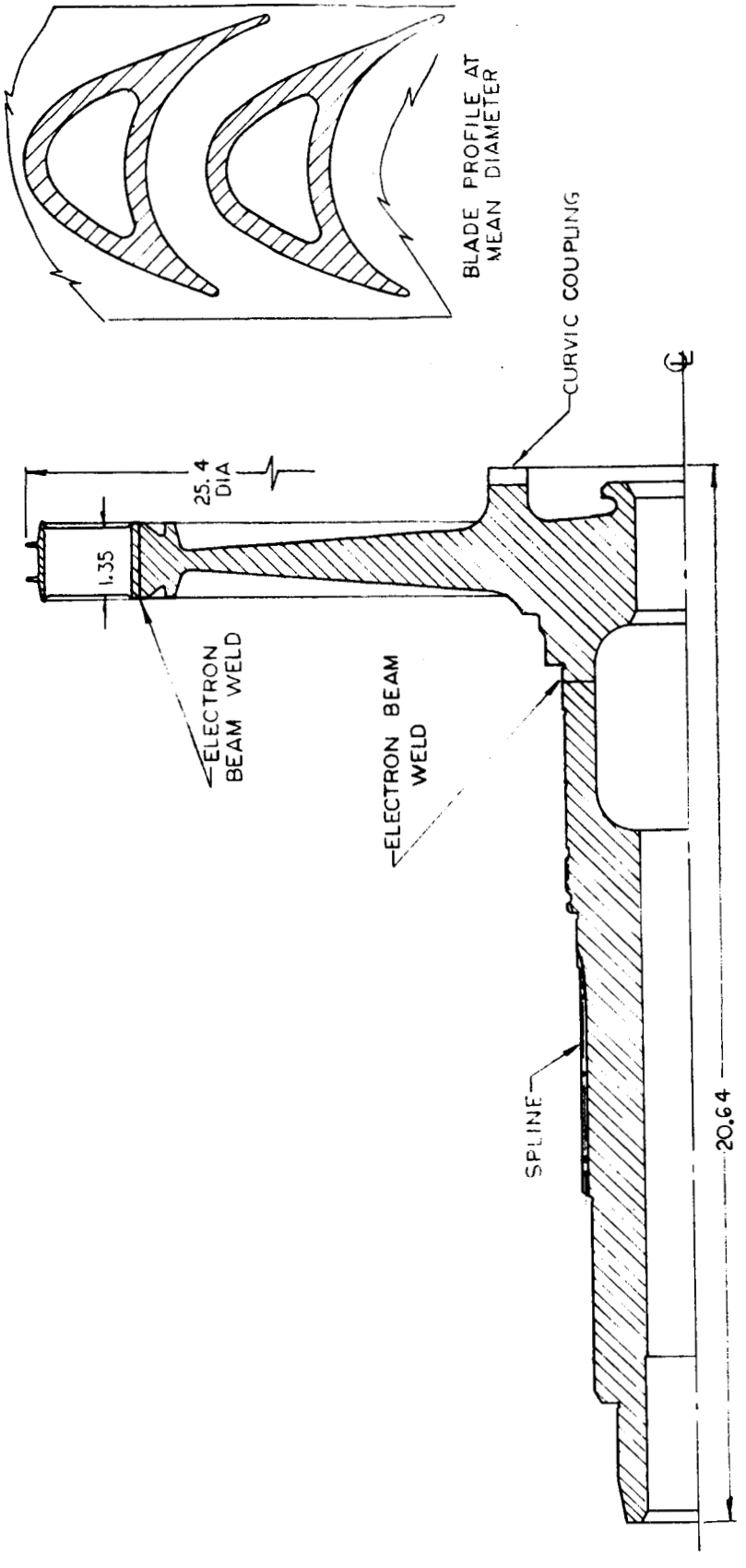


Figure 3

First-Stage Rotor and Blades

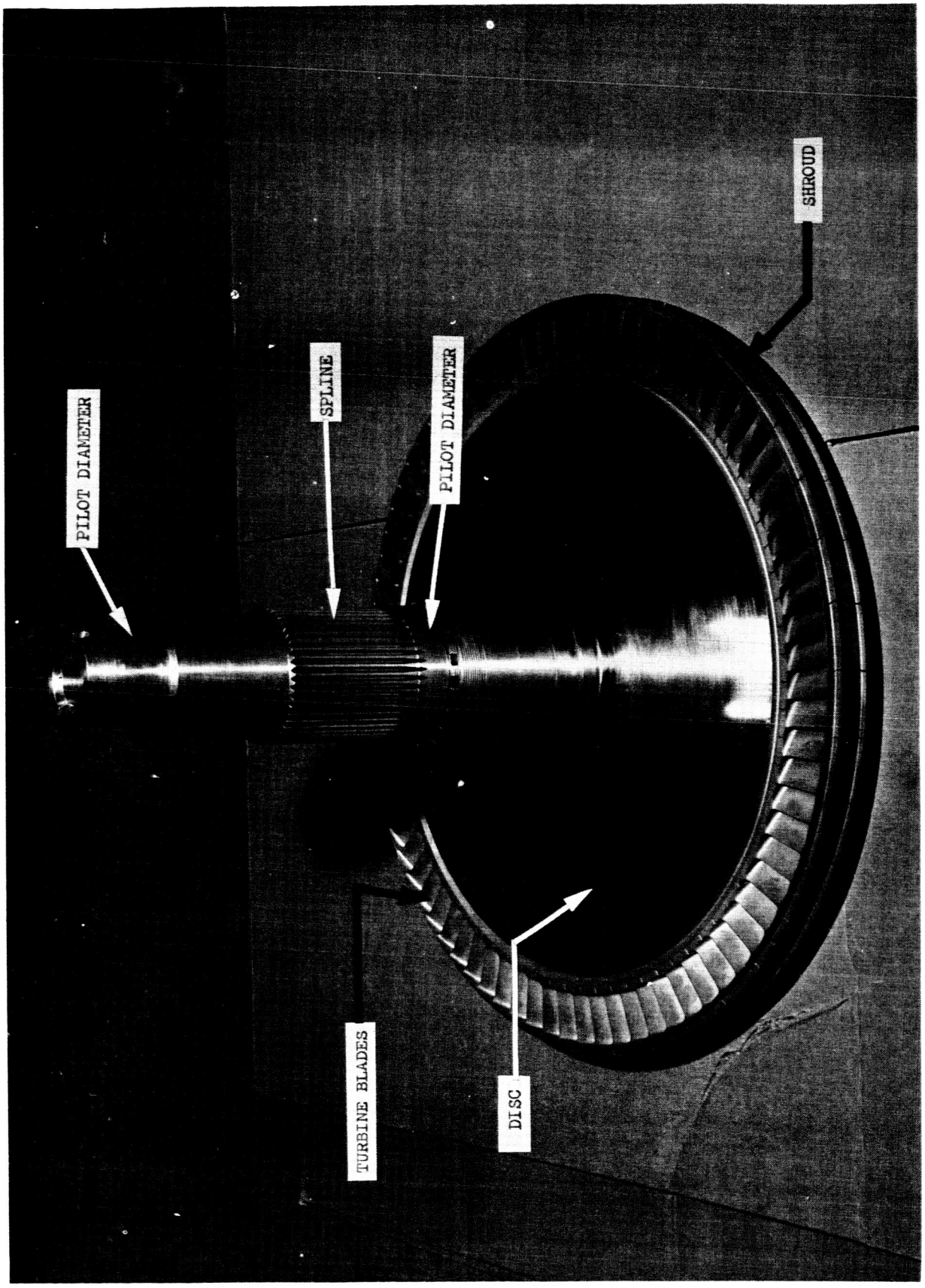


Figure 4

First-Stage Rotor - Front Side

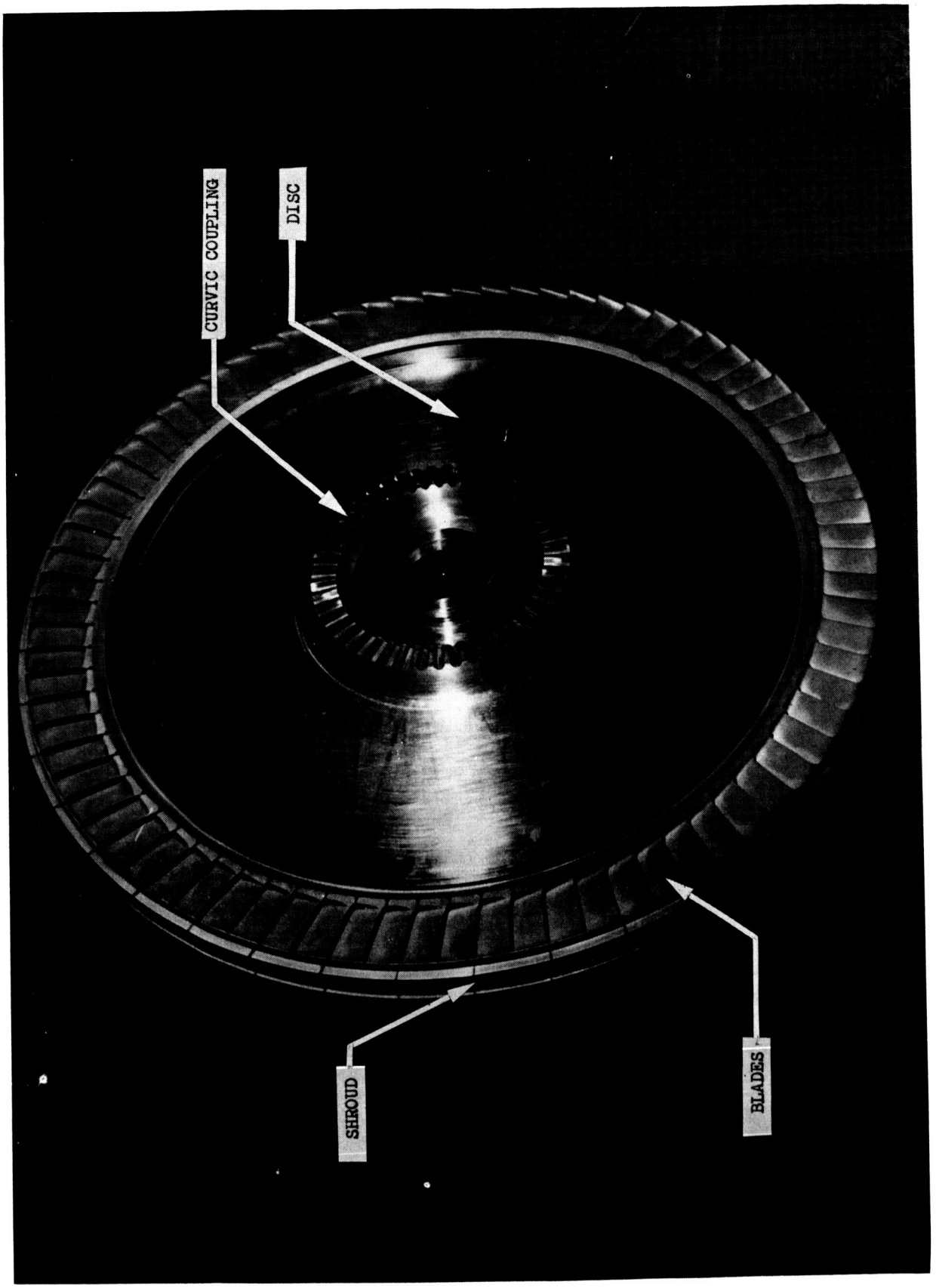


Figure 5

First-Stage Rotor - Aft Side

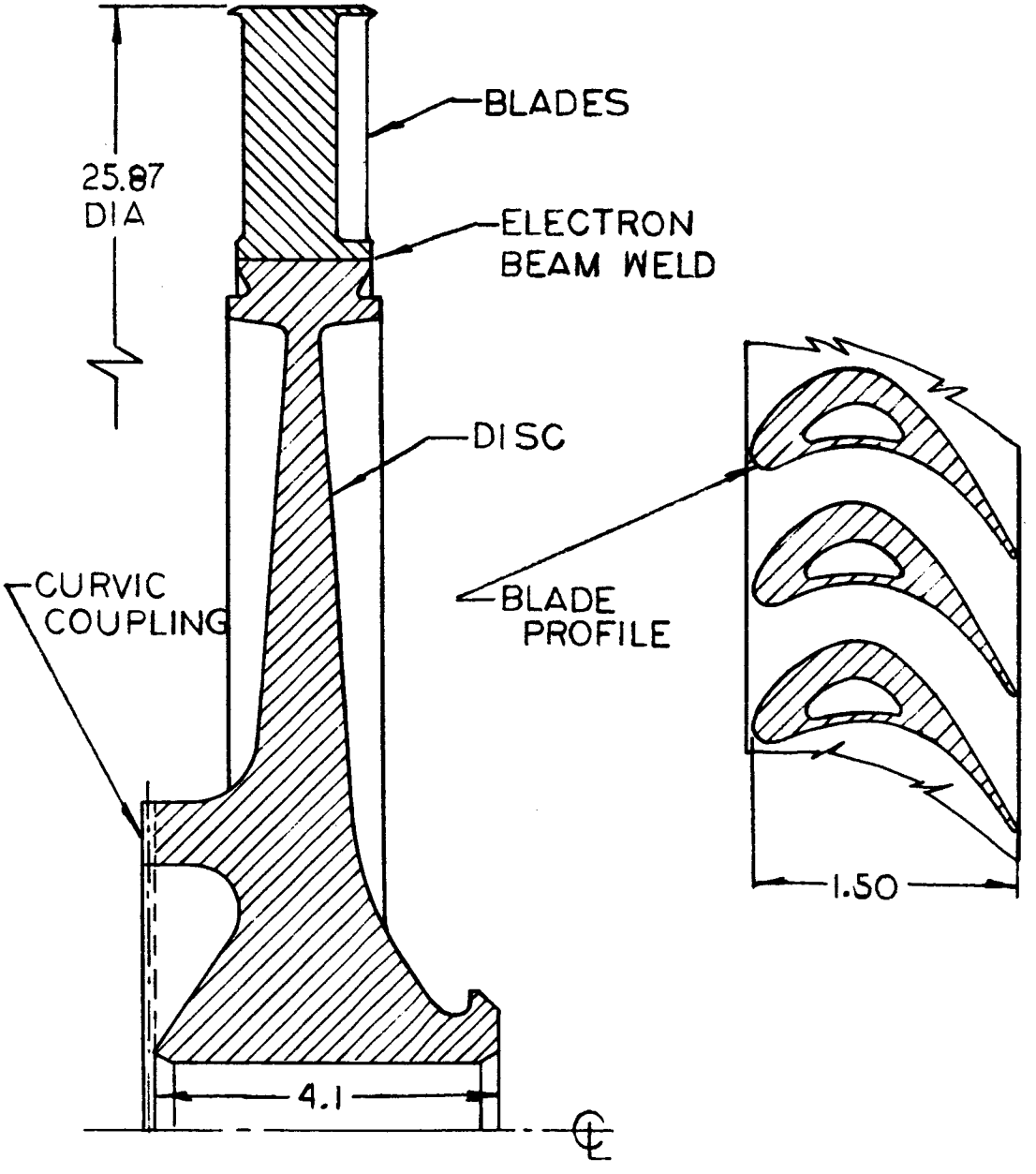


Figure 6

Second-Stage Rotor and Blades

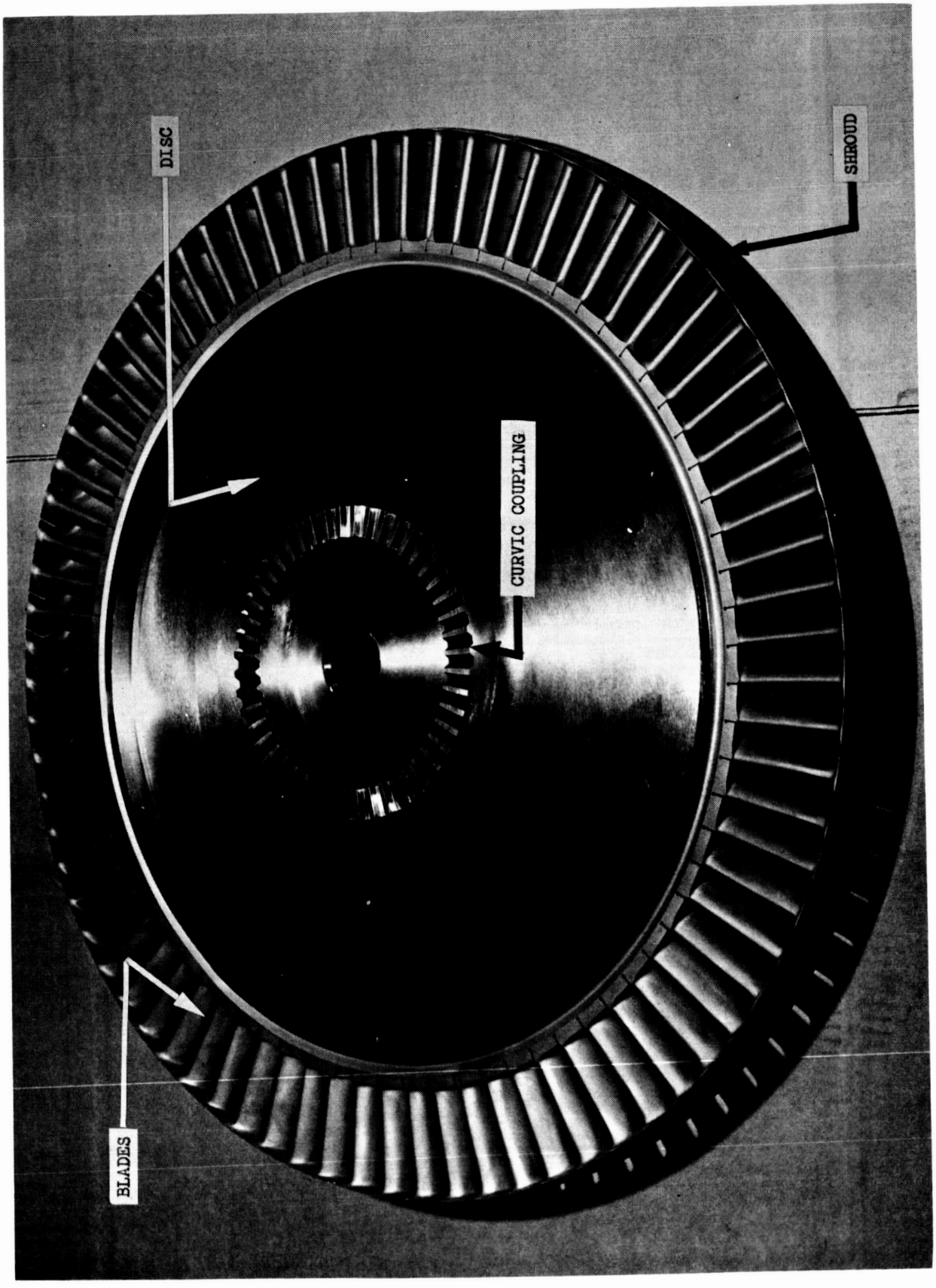


Figure 7

Second-Stage Rotor - Front Side

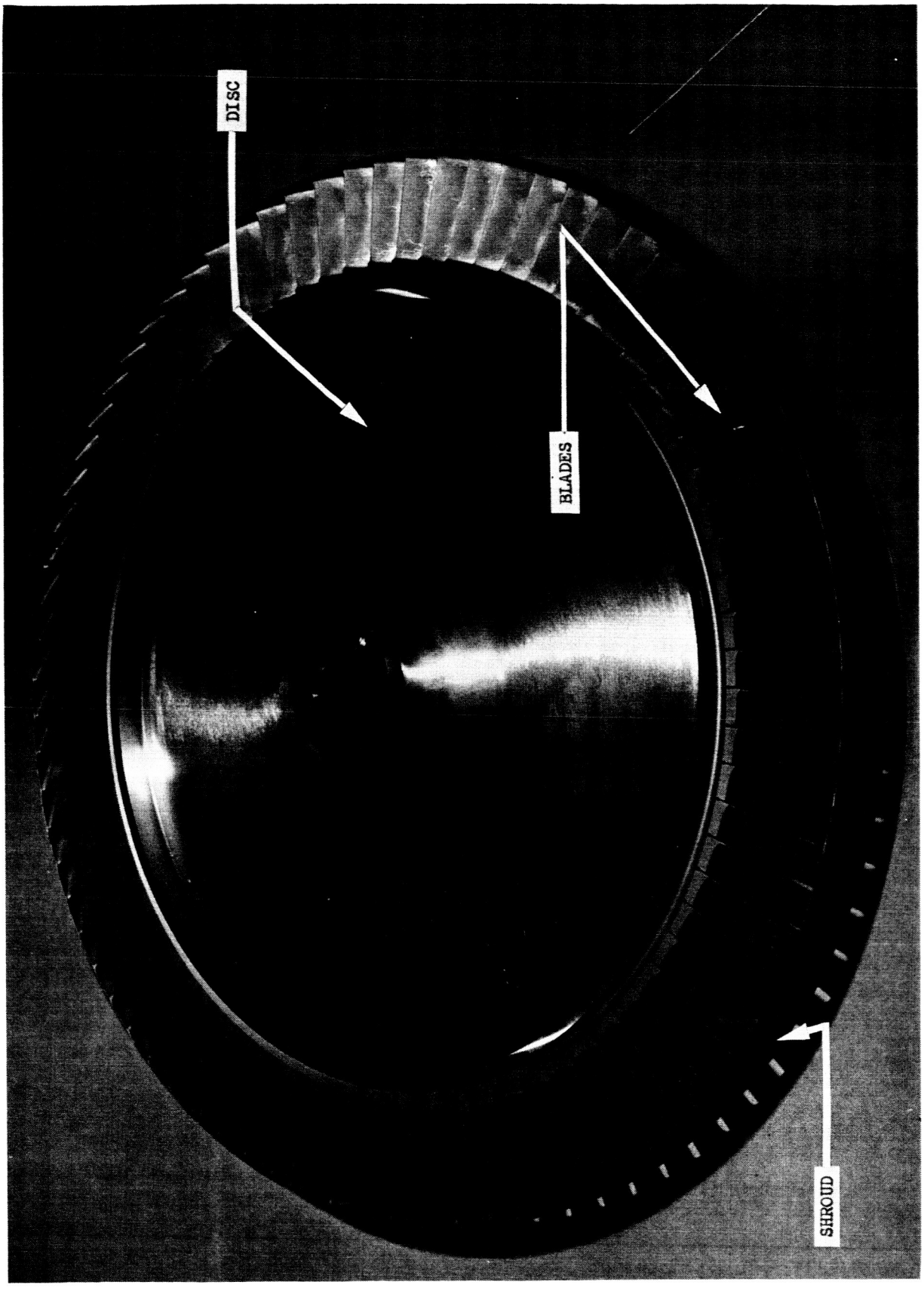


Figure 8

Second-Stage Rotor - Aft Side

to the pump discharge housing by means of the space frame shown in Figure No. 2. This frame consists of three equally spaced conical sections, to provide openings for the inlet manifold and instrumentation lines. A support frame section is shown in Figure No. 9. The housings are supported at a single main flange, which is positioned near the axial center of the blades rows. This location allows thermal movements in all directions with the least affect upon axial clearances between the rotating and the stationary members. The turbine housing joint consists of lightweight flanges secured by clamps. Sealing is accomplished by applying a small weld bead to the flange joint before the clamps are installed.

The inlet manifold consists of a constant cross-sectional area torus having a nozzle ring in one side as shown in Figure No. 10. The nozzle ring has 37 vanes, which can be seen in Figure No. 11. A flow deflector consisting of a flat plate shaped to fit the inlet is inserted in the inlet neck to reduce gas turbulence around the protruding outer nozzle shroud. In general, the parts are fabricated from sheetmetal for minimum weight and to allow thermal movement resulting from temperature changes.

The reversing row has 67 vanes and is installed between the first-stage and second-stage rotors. This reversing row is made up of six circular segments to permit unrestricted movement under the varied thermal conditions encountered during pump chilldown and operation. The vane segments are of sheetmetal construction. The reversing vanes are shown in Figure No. 12. The segmented ring is mounted on its outer diameter by clamping it between the inlet manifold and the exhaust housing.

There are two types of turbine exhaust housings. The turbopump test unit shown in Figure No. 13 is a single outlet, conical housing which connects to the turbopump test stand exhaust ducting. The engine turbopump unit shown in Figure No. 14 is a hemispherical, dual outlet housing which connects to the crossover ducts that carry exhaust gases to the M-1 liquid oxygen turbopump turbine. The dual exit exhaust housing includes a connection for the 5-in. turbine by-pass duct and has an access pad which can be removed to manually torque check the turbopump rotor. During engine operation, flow in the turbine by-pass duct would be controlled to provide engine calibration as well as to provide propellant utilization control.

2. Method for Achieving Mechanical Design Objectives

The turbine inlet manifold is a combined torus, nozzle assembly, and turbine casing. These components are welded into one assembly giving a lightweight, strong structure that is free to move with the large thermal gradients.

The housings are supported from a main flange that is located near the axial center of the blade rows. This permits unrestrained thermal movement of the static turbine housings without seriously affecting blade row alignment and clearances. The support frame attaches on the outside diameter of the

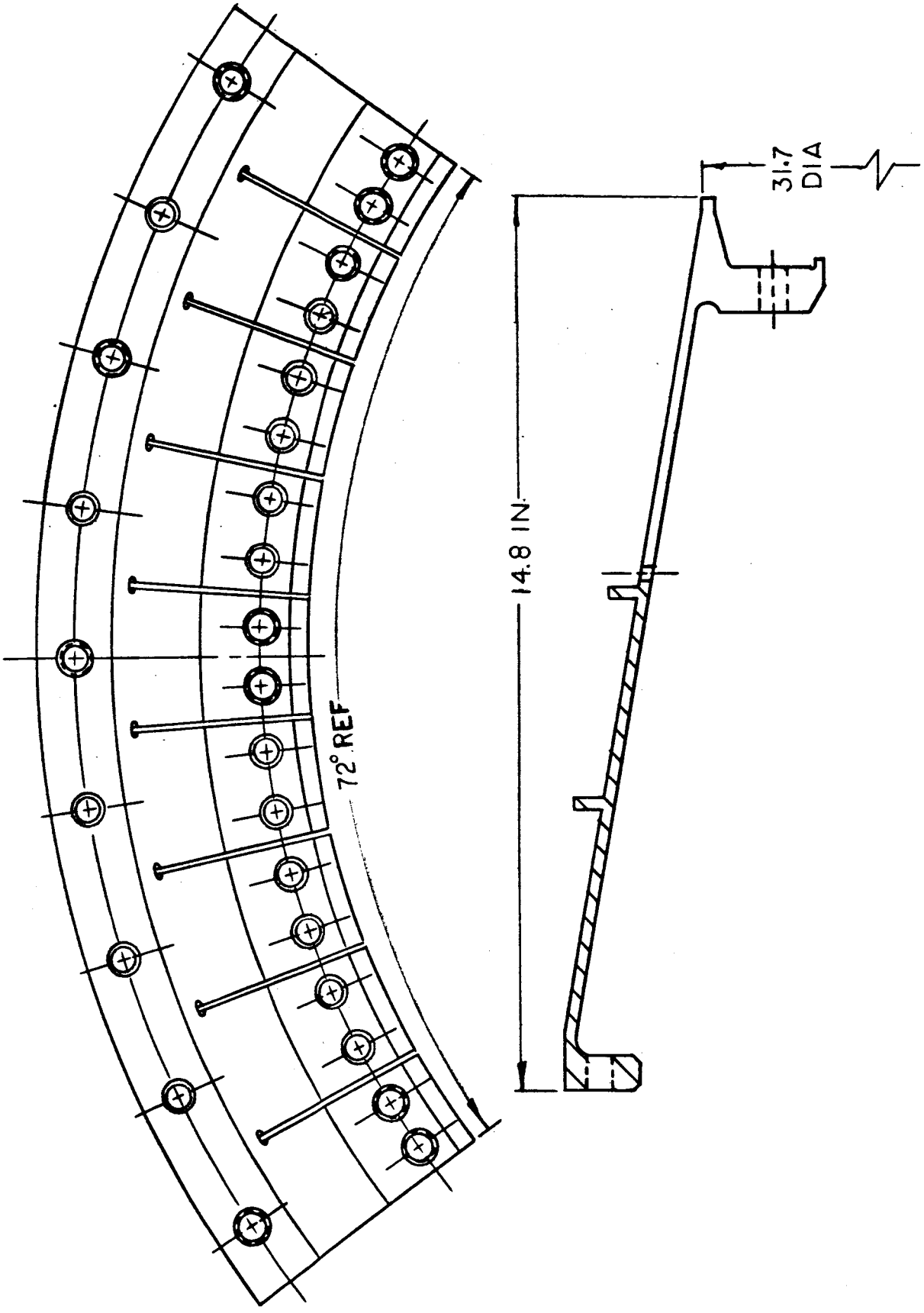


Figure 9

Turbine Support Frame

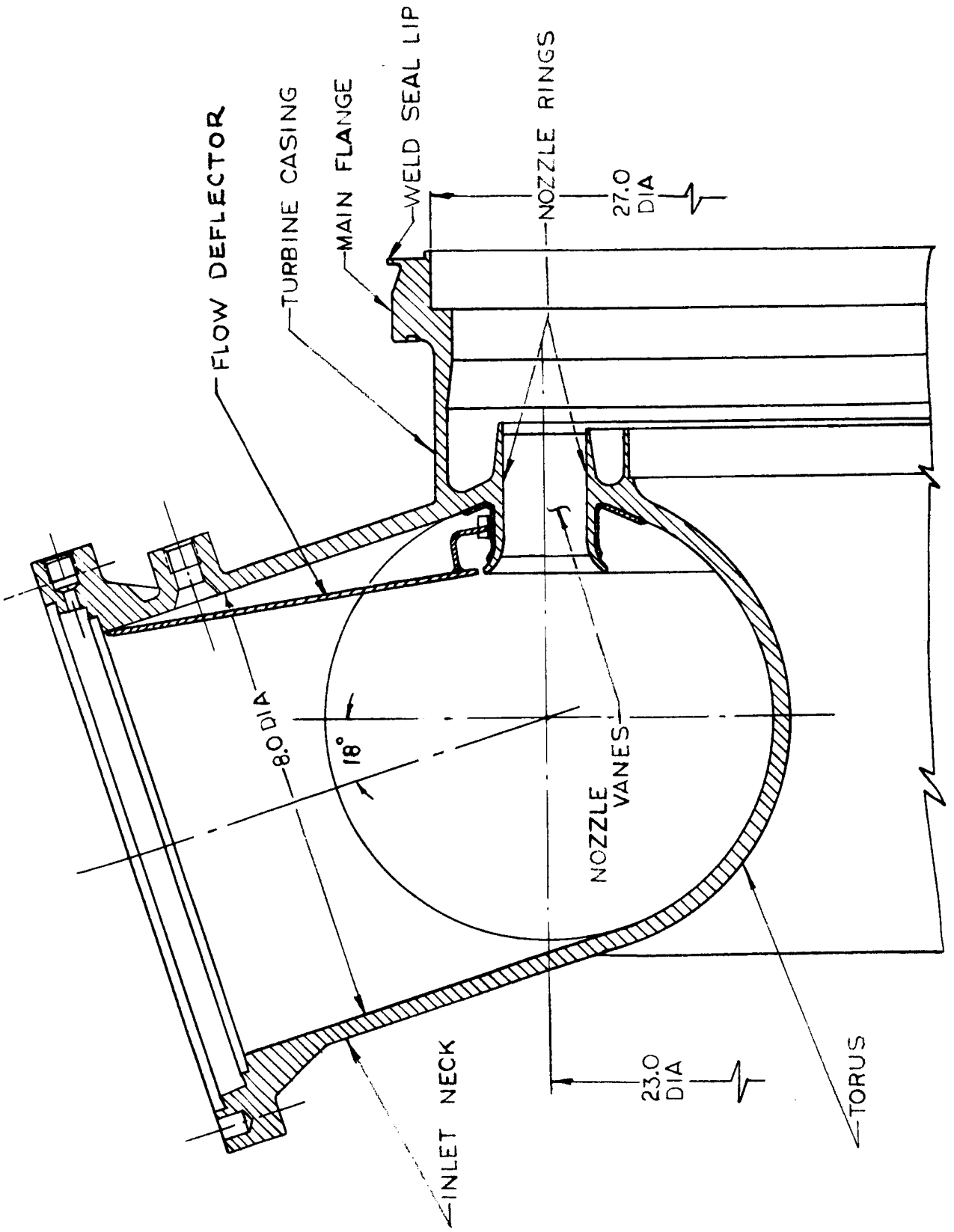


Figure 10

Torus and Nozzle Assembly

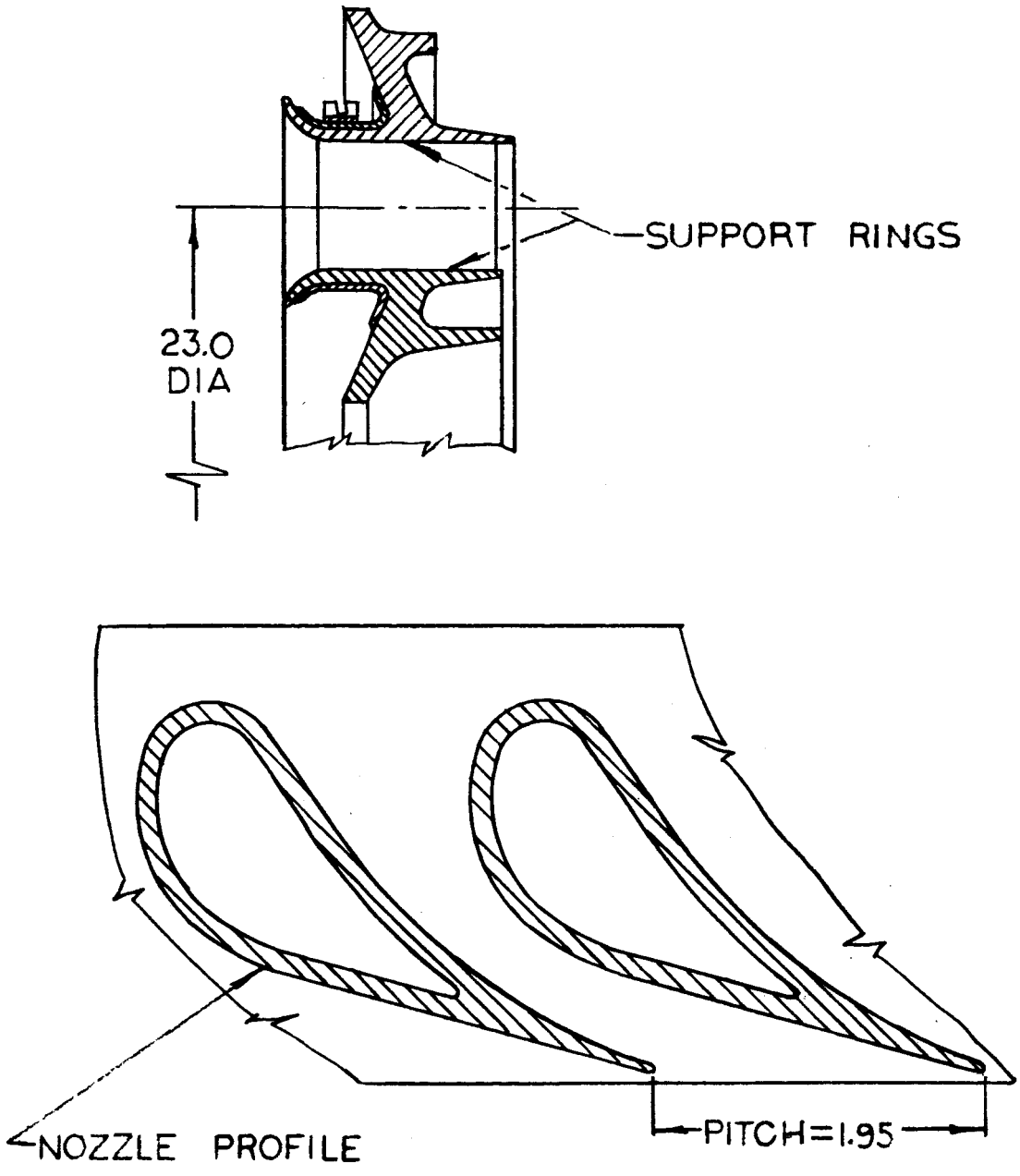


Figure 11

Nozzle Profile and Support Rings

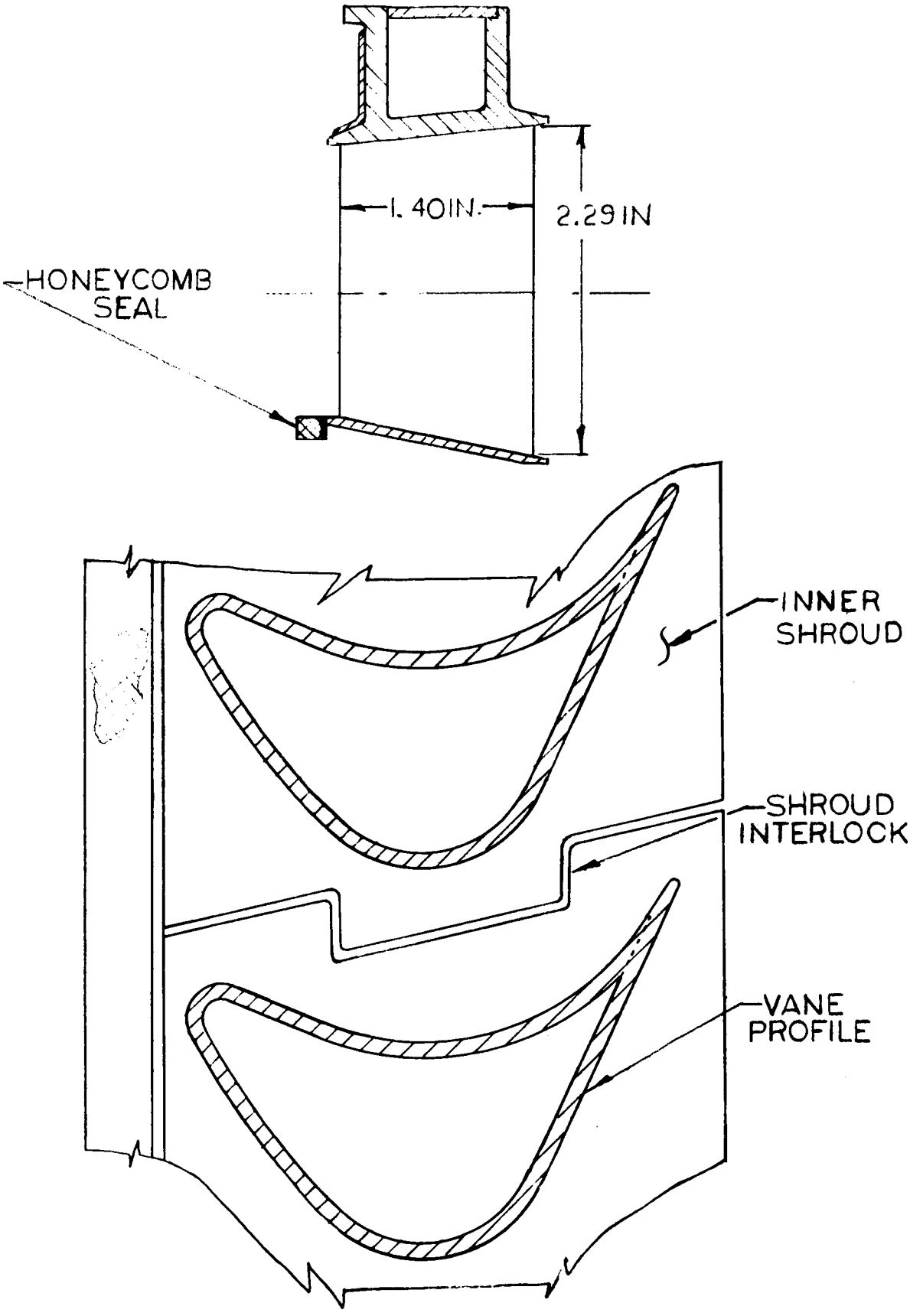


Figure 12

Reversing Row, Section and Vane Profile

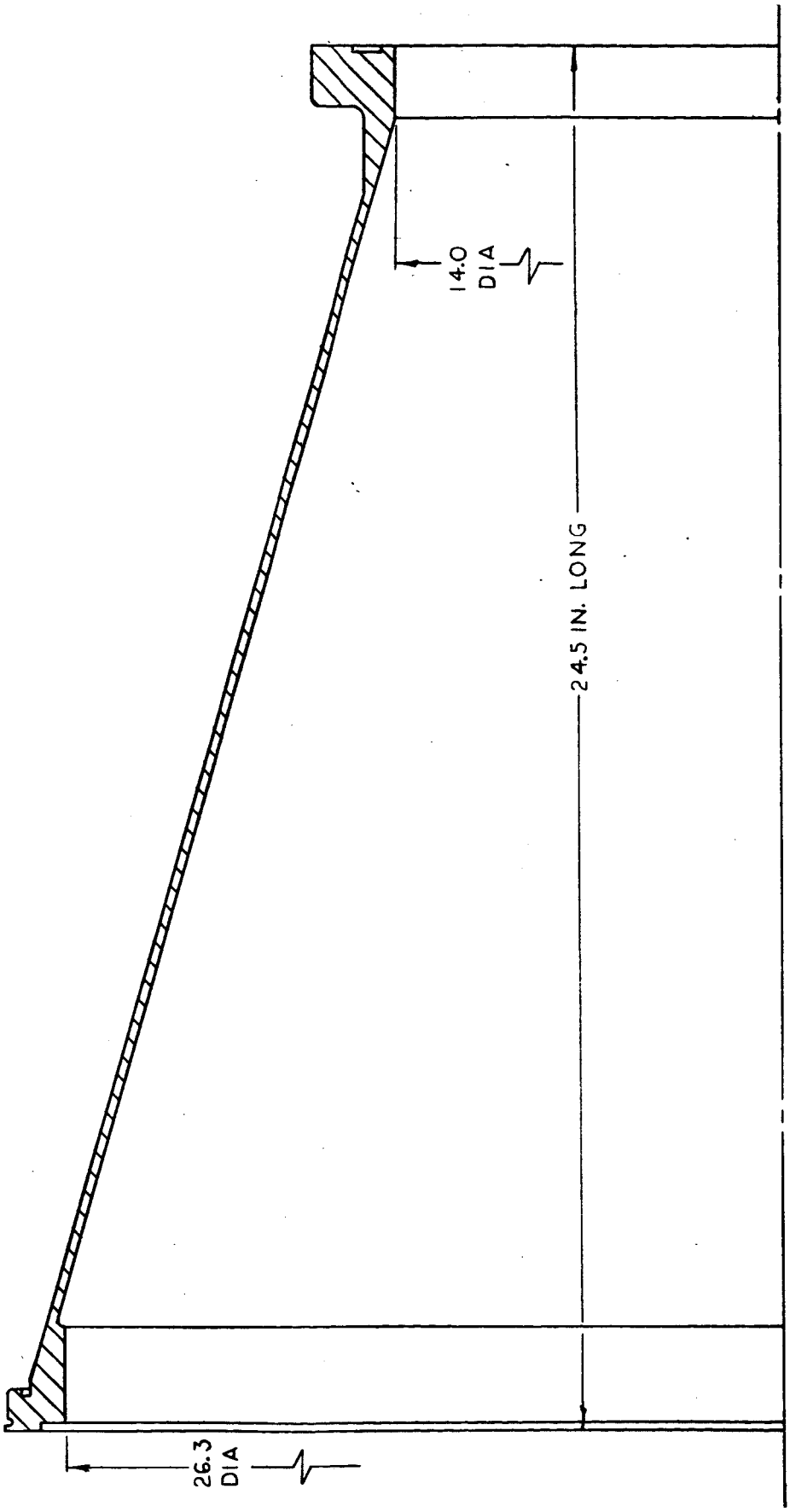


Figure 13

Turbine Exhaust Cone

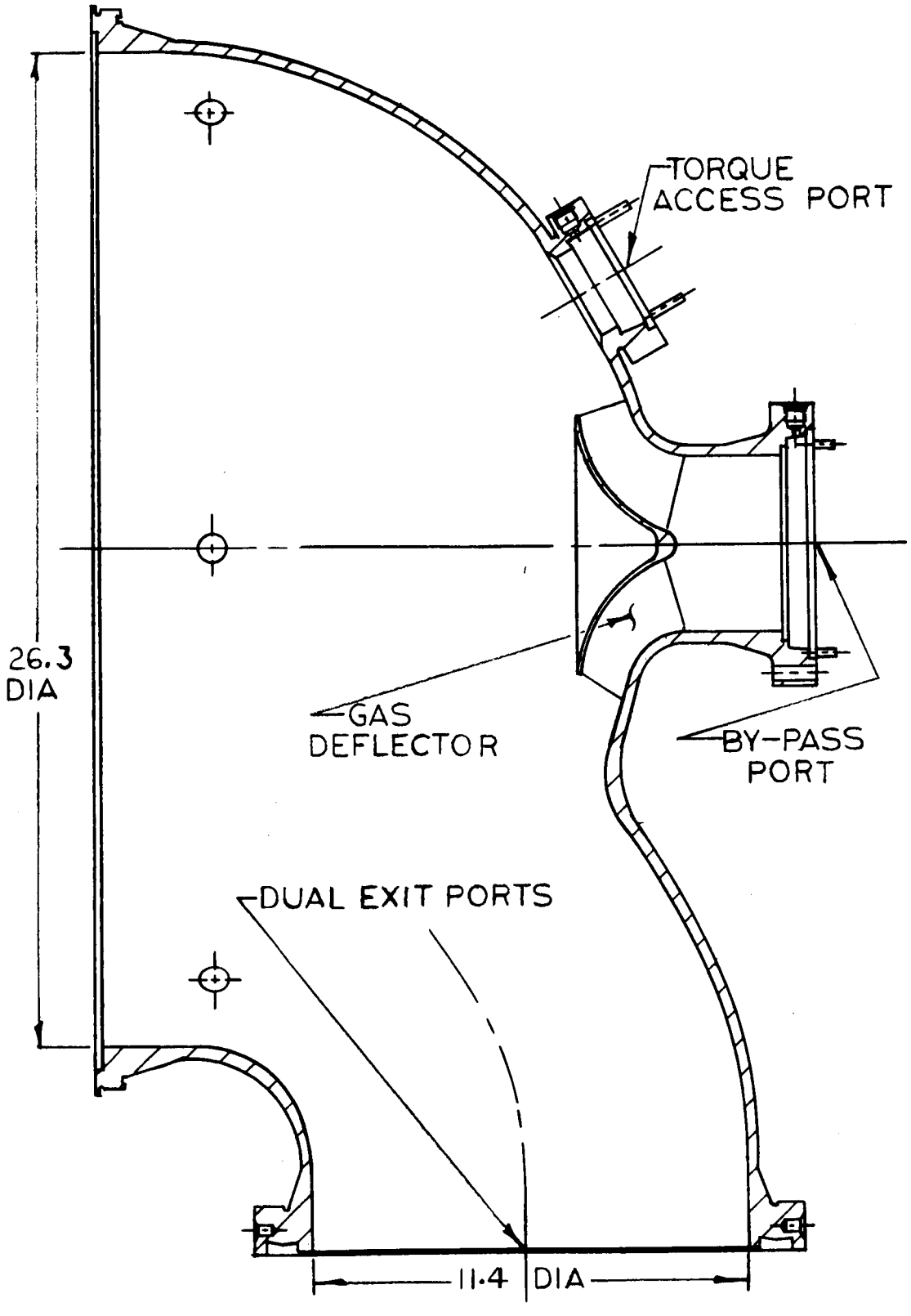


Figure 14

Dual Exit Exhaust Housing

main flange and extends back to the pump housing. This frame is free to move radially at the turbine end to allow for contractions and expansions of the turbine housings. To reduce weight and thermal distortions, the main flange is held together and attached to the support frame by means of clamps. A small (.060-in.) weld beam is applied to the flange joint to seal against hot gas leakage.

A 17.5-in. shaft was welded to the first-stage turbine rotor to allow close coupling of the turbine-end bearing. It also simplifies the assembly with the pump rotor and seal assembly. Piloting journals and a spline are provided for alignment and power transmission. The opposite end has a curvic coupling for centering and transmitting torque from the second rotor.

Attachment of the two hot turbine rotors to the cold pump rotor was accomplished by use of a long, elastic tie-bolt. This allows thermal contractions and expansions during transient conditions without overstressing the parts.

The turbine blades were forged to obtain good material strength and to allow for an integral shroud on the outside diameter, which improves performance and permits blade vibration control. The blades have internal cavities to reduce weight and improve thermally-induced stresses. These blades are attached to the discs by electron-beam welding, which reduces the disc rim thickness, and resultant weight as compared with the mechanical attachment methods.

To permit unrestricted thermal movement during temperature transients, the reversing row is divided into six segments and retained in the main housing flange with a groove and tongue arrangement. Leakage around the inside diameter of the reversing row is controlled by a honeycomb seal that is positioned close to the first rotor rim.

### 3. Basis for Configuration Selection

Series flow turbine sets for the M-1 liquid hydrogen and liquid oxygen turbopumps were selected over parallel flow turbine sets upon the bases of engine performance and turbopump complexity criteria. Parallel flow turbine sets result in either an increased gas generator weight flow or an increased number of turbine stages.

Because of the higher power and shaft speed requirements of the liquid hydrogen turbopump, the liquid hydrogen turbopump turbine set was selected to be the higher pressure set. This assured that turbine rotor stress levels would be acceptable for both the liquid hydrogen turbopump turbine set as well as the liquid oxygen turbopump turbine set.

Single-stage, two-stage, and three-stage turbines were considered for the liquid hydrogen turbopump set. The two-stage was selected over

the single-stage using engine performance and weight as the basis. The two-stage turbine reduces gas generator weight flow, thereby increasing engine specific impulse performance. Based upon typical vehicle payload comparisons, the increase of engine performance for the two-stage turbine version more than offset the engine weight increase for the second stage.

The two-stage turbine was selected over a three-stage turbine because the payload increase resulting from the increased engine performance of the three-stage version is nearly offset by the third stage weight increase. Also, the three-stage turbine turbopump requires an aft or outboard bearing to achieve shaft critical speed requirements; whereas, the two-stage turbine turbopump achieves shaft critical speed criteria with a forward or inboard bearing arrangement. The aft bearing would increase turbopump complexity by requiring additional bearing coolant circuits, bearing coolant circuit control valving, and a special turbine structure for the support and alignment of the aft bearing.

A velocity-staged turbine was selected in preference to a pressure-staged turbine because the second-stage stator blade and diaphragm of the velocity-staged turbine is lighter and simpler. For the specified operating conditions, turbine efficiencies for the velocity-staged and pressure-staged turbines are essentially equal.

Impulse blading was selected in preference to reaction blading for the first-stage because the impulse blading gave higher efficiency for the design conditions. Also, the impulse blading gives lower turbine housing pressure which minimizes turbine housing weight. The second-stage stator (reversing blade row) and the second-stage rotor have slight reaction flow to sufficiently accelerate the flow to offset frictional losses.

## C. MATERIAL SELECTION

### 1. Material Requirements

To meet the mechanical design point conditions as well as the design considerations, the turbine materials should have the following qualities:

a. High strength at operating temperatures to permit thin cross-sections.

b. Good elongation characteristics over a wide range of temperatures, (-420°F to +1300°F) to withstand thermal shock, facilitate crack-free welding, and permit localized yielding.

c. Good stress-rupture properties up to 1300°F.

d. Corrosion resistance.

e. Reasonable machinability and metal-forming qualities.

f. Be suitable for welding by gas tungsten arc welding or electron-beam method.

g. Capable of being annealed for stress relief and heat treated for maximum strength.

2. Selected Materials

A comparatively new material that conformed to these requirements was selected for most components of the M-1 fuel turbine. This material, Inconel 718, is a nickel-chromium alloy that is age-hardenable. Its material properties are as follows:

a. For stress-rupture limited applications, the material is solution-annealed at 1800°F. It is aged at 1325°F and 1150°F with the following properties:

(1) For bars and forgings, 23 hours life at 1300°F and 75,000 psi stress.

(2) For sheet and plate, 23 hours life at 1300°F and 72,500 psi stress.

b. For tensile-limited applications of ambient to above 1200°F, the material is solution-annealed at 1950°F. It is aged at 1350°F and 1200°F with the following properties:

(1) The room temperature-tensile, ultimate and yield strengths are 175,000 psi and 145,000 psi, with minimum elongations of 12%.

(2) The 1200°F tensile, ultimate, and yield strengths are 145,000 psi and 125,000 psi, with minimum elongations of 10%

Rene' 41 was selected for the first-stage rotor shaft extension, mainly because its coefficient of thermal contraction was slightly less than Inconel 718. This factor permitted tolerances in the turbine journals so they would assemble into the pump rotor with a slightly loose fit at room temperature. At -420°F, the pump rotor will contract around the Rene' 41 shaft producing an interference-fit joint. Also, this material has good mechanical properties and can be welded to the 718 turbine rotor.

Another factor in selecting Rene' 41 for the shaft concerned the turbine bearing inner race fit. The inner race is of 440C stainless steel and had a significantly lesser contraction at -420°F than 718, but it is closer to the contraction rate of Rene' 41. This allowed a smaller room temperature

interference-fit.

D. STRUCTURAL CRITERIA

1. Static or Non-Rotating Components

The static and non-rotating components were designed with the following minimum criteria:

a. Proof pressure (yield) = 1.2 (factor of safety) times Po, where Po equals the maximum static pressure expected to exist at any time.

b. Burst pressure (ultimate) = 1.6 (factor of safety) times Po.

c. The safety factors from nominal working pressures for flexible hoses, tubing, and pressure fittings with diameters less than 1.5-in. are 2.0 for proof and 4.0 for burst.

d. Pressure vessels are designed to withstand 500 operating pressure cycles.

e. Proof and burst pressures for tests at ambient temperatures are adjusted to compensate for material strengths at operating temperatures. Proof pressure is that test pressure to which an item is subjected for a minimum of two minutes without deformations that adversely affect the rocket engine.

f. In addition to the above safety factors, a factor of 1.15 shall be used for all fittings, mounts, and bolts which either constitute the only load path or whose failure would interfere with the proper functioning or integrity of any engine component.

The section areas were determined using the material strength at the maximum expected operating temperature. For most parts, the ultimate strength was used as the limiting structural criteria. The margin of safety is defined as follows:

$$M.S. = \frac{\text{Allowable Stress}}{\text{Calculated Stress}} - 1$$

In general, the calculated stress includes the applicable safety factor.

The fatigue margin of safety is applied to components having a fluctuating stress and is determined by use of a modified Goodman diagram. For these calculations, the alternating stress is assumed to be 30% of the maximum mean stress. The fatigue margin of safety is calculated as follows:

$$M.S. = \frac{\text{Allowable Stress From Goodman Diagram}}{1.25 \times \text{Calculated Stress}}$$

This calculation includes a 1.25 safety factor.

2. Rotating Components

Rotating components were designed with the following minimum criteria:

a. Design Yield = 1.0 (Factor of Safety) times limit load, where limit load is the maximum predicted load which the system may experience under specified operating conditions.

b. Design Ultimate = 1.5 (Factor of Safety) times limit load.

c. Components subjected to elevated temperatures shall be designed using material properties at the estimated maximum temperature environment.

d. The fatigue margin of safety is applied to components having a fluctuating stress and is determined by use of a modified Goodman diagram. The alternating stress is assumed to be 30% of the maximum mean stress. The fatigue margin of safety, which includes a 1.25 factor of safety, is calculated as follows:

$$\text{M. S.} = \frac{\text{Allowable Stress from Goodman Diagram}}{1.25 \times \text{Calculated Stress}}$$

The turbine blade limiting stress was determined by adding centrifugal, gas bending, and assumed alternating stress at 110% of operating speed to determine the fatigue margin of safety. Margins of safety included the effect of transient thermal stresses.

The turbine rotor design was based upon symmetrical sections of constant stress, except at the neck (just below the blade platform) and the bore. The neck area is sufficiently reduced to permit inducer blade shedding prior to disc failure. The bore stress was limited to less than twice the yield strength at the local temperature. The average tangential stress in the disc was limited by a 2.0 safety factor upon the ultimate strength. Transient thermal-induced stresses were superimposed upon the combined stresses to obtain calculated margins of safety.

3. Vibration and Acceleration Loads

Operation at a point which will excite the natural frequency or some harmonic of a component should be avoided unless the vibration-induced load is below the design criteria.

The engine-induced, flight acceleration loads within the turbine design are as follows:

| | | |
|---|---|---|
| a. | Longitudinal | 10 g |
| b. | Lateral | 1 g |
| c. | Angular | 1.5 Rad/Sec$^2$ |
| d. | Gimbal snubbing | 20 Rad/Sec$^2$ |

E. COMPONENT STRESS SUMMARY

1. Turbine Inlet Manifold

The maximum stresses produced from the shock loading and from the 2½ g vibratory line loads do not occur at the same locations as the maximum stresses from gas pressure and thermal gradients. Shock load produces a moment on the inlet nozzle. This load occurs during an emergency shutdown when the end of the inlet duct is blown-off to rapidly release turbine supply pressure. The controlling stresses are those produced from gas pressure and thermal gradients. Figure No. 15 shows the gas temperature transient to which the torus and nozzles are exposed.

The structure is analyzed by use of an Aerojet-General Corporation computer program (Job No. 1040)(4).

The analysis shows that yielding will not be the critical mode of failure. Fatigue will cause failure after 2200 starts.

A tabulation of inlet manifold stresses with 1175 psi internal pressure and a steady-state temperature of 1300°F is shown in Figure No. 16.

The most severe stress case with 1175 psi internal pressure and the maximum transient thermal gradient is shown in Figure No. 17.

The calculated stresses developed using the required fixturing for hydrotesting, which imposes different loads at some points, are tabulated in Figure No. 18.

A tabulation of the stresses with 1175 psi internal pressure, a temperature of 1300°F, with 2½g line loads applied, and the blow-off valve shock load imposed, are shown in Figure No. 19.

(4) This program was devised from information in the paper, A Numerical Analysis of the Equations of Thin Shells of Revolution, by Radkowski, P. P., Davis, R. M., and Boldul, M. R., Avco Corp.

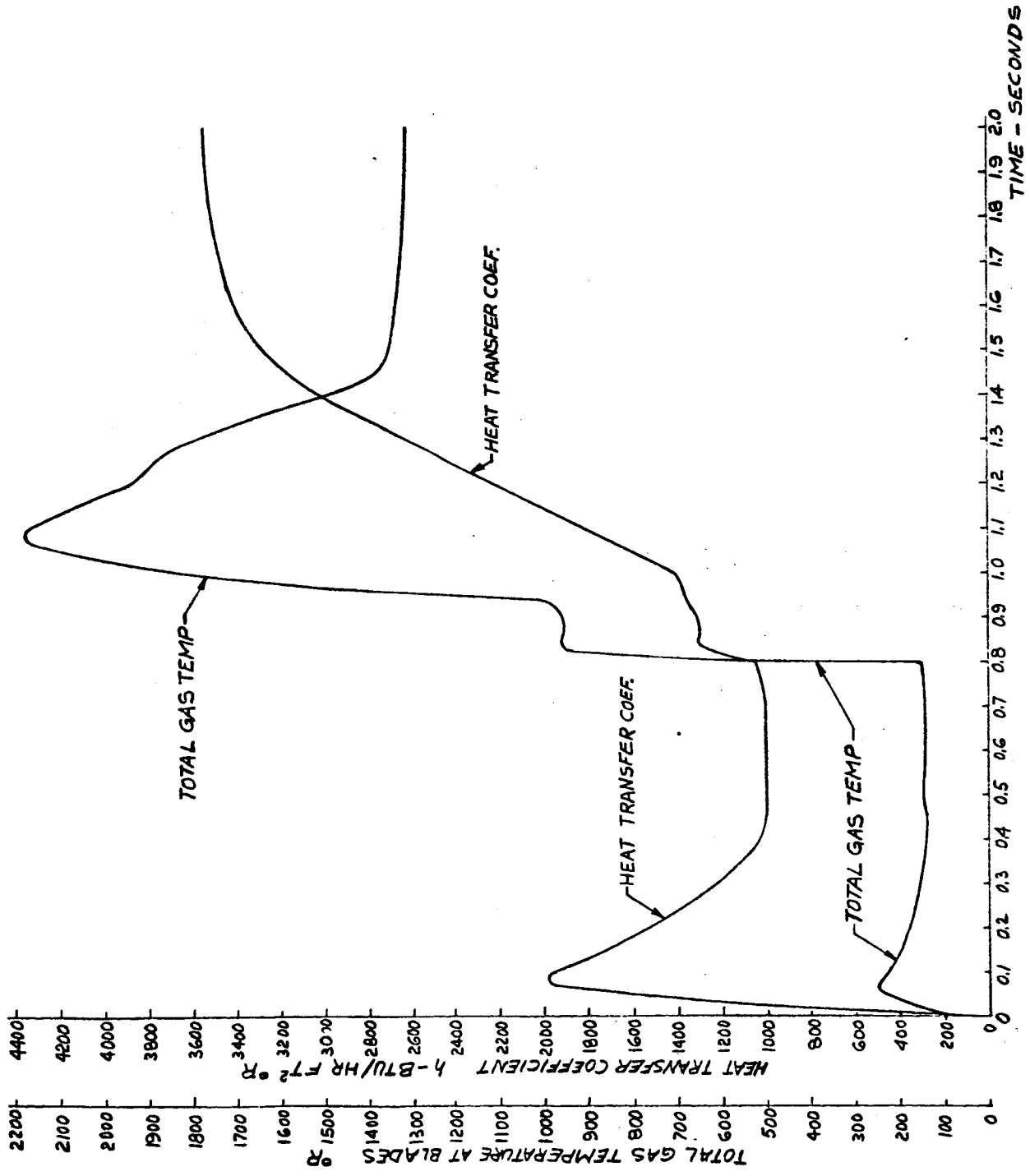


Figure 15

Gas Temperature Transient at Startup

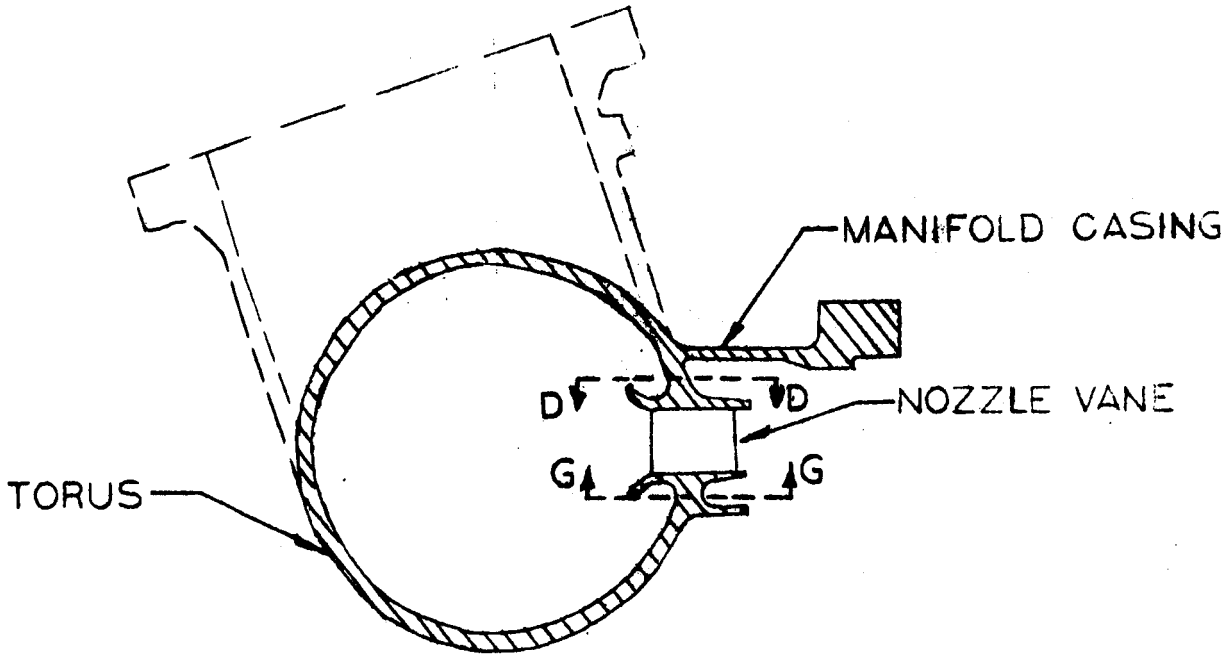


PRESS. STEADY = 1175 psi  TEMP. STEADY = 1300° F

| LOCATION | MAX. BENDING STRESS | MAX. DIRECT STRESS | MARGIN OF SAFETY |
|---|---|---|---|
| SEC. D-D | 56,700 | 27,000 | 0.16 |
| SEC. G-G | 72,500 | 41,800 | -0.165* |
| NOZZLE VANE | 21,200 | 10,850 | 2.00 |
| MANIFOLD CASING | 67,400 | 5,660 | 0.44 |
| TORUS | 43,380 | 35,190 | 0.18 |

*FATIGUE FAILURE AFTER 6700 CYCLES

Figure 16

Inlet Manifold Stress, Steady-State

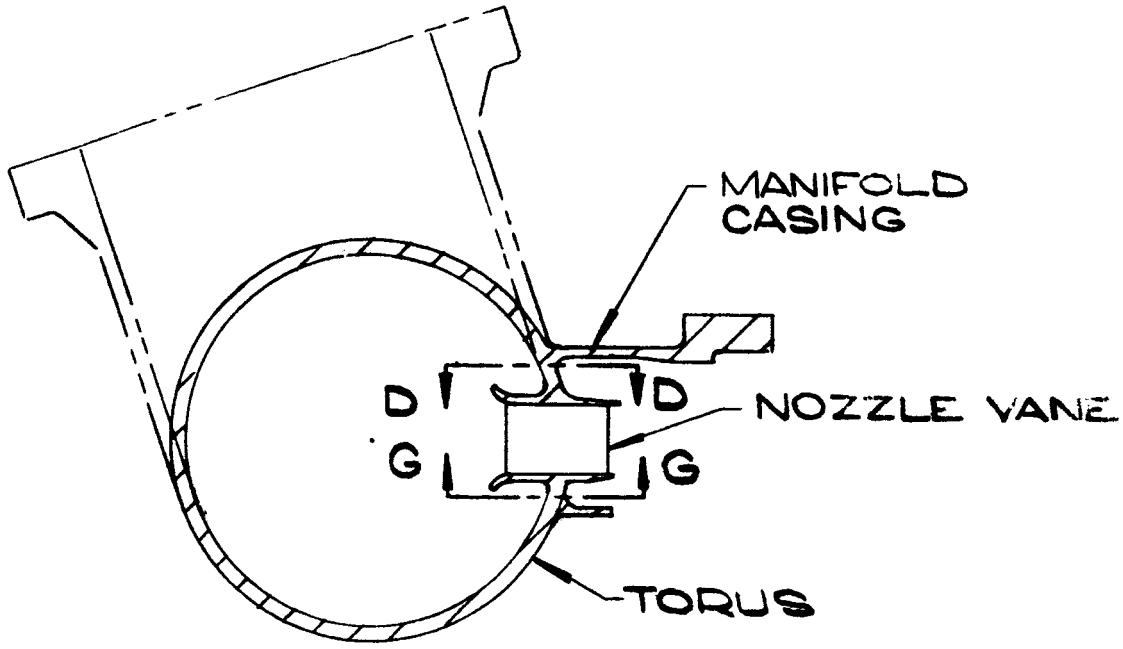


DRESS. STEADY: 1175 PSI, MAX THERMAL GRADIENT

| LOCATION | MAX BENDING STRESS | MAX DIRECT STRESS | MARGIN OF SAFTEY |
|---|---|---|---|
| SEC. D-D | 8,700 | 6,200 | HIGH |
| SEC. G-G | 101,900 | 60,700 | -0.395 * |
| NOZZLE VANE | 33,300 | 10,850 | 0.98 |
| MANIFOLD CASING | 63,600 | 5,660 | 0.55 |
| TORUS | 61,780 | 25,360 | 0.40 |

* FATIGUE LIFE: 2,200 CYCLES

Figure 17

Inlet Manifold Stress, Maximum Thermal Gradient

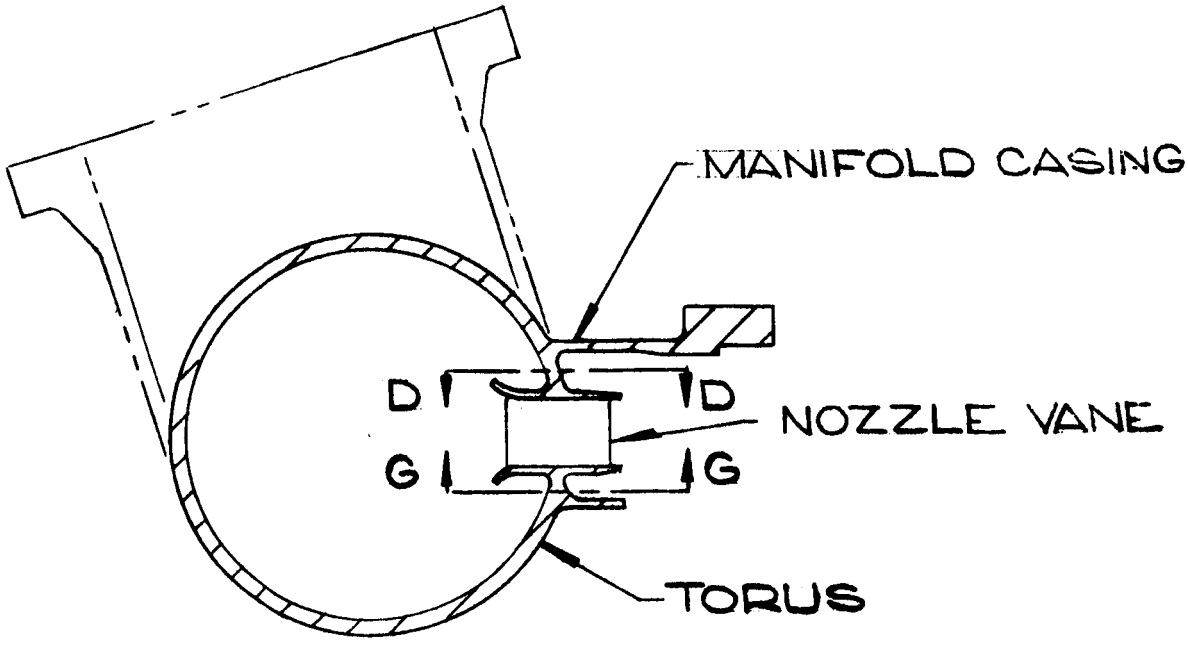


MAX INTERNAL PRESSURE = 1275 PSI

| LOCATION | MAX BENDING STRESS | MAX DIRECT STRESS | MARGIN OF SAFETY 1.6 F.S. | MARGIN OF SAFETY ZERO F.S. |
|---|---|---|---|---|
| SEC D-D | 111,700 | 19,500 | 0.15 | 0.64 |
| SEC G-G | 156,000 | 49,000 | -0.27 | 0.18 |
| NOZZLE VANE | 46,200 | 13,100 | 0.90 | HIGH |
| MANIFOLD CASING | -194,000 | 17,500 | -0.24 | 0.22 |
| TORUS | 136,780 | 37,560 | -0.13 | 0.40 |

Figure 18

Inlet Manifold Stress, Proof-Pressure Test

| LOCATION | 2½ G VIBRATION AND SHOCK LOAD STRESS PSI | ADDITIONAL DUE TO 1175 PSI AT 1300°F PSI | COMBINED PSI | MARGIN OF SAFETY |
|---|---|---|---|---|
| SECTION G-G | NEGLIGIBLE | 72,500 BEND<br>41,800 DIR | 72,500 BEND<br>41,800 DIR | -0.165* |
| SECTION D-D | NEGLIGIBLE | 56,700 BEND<br>27,000 DIR | 56,700 BEND<br>27,000 DIR | +0.16 |
| INLET NECK | 35,800 | 14,100 | 49,900 | 0.56 |
| MANIFOLD CASING | 14,400 BEND<br>26,700 DIR | 67,400 BEND<br>5,660 DIR | 81,800 BEND<br>32,60C DIR | -0.14* |
| TORUS | 10,400 SHEAR AND TENSION | 43,380 BEND<br>35,190 DIR | 43,380 BEND<br>45,590 DIR | 0.02 |

* FATIGUE LIFE = 6,700 CYCLES




Figure 19

Inlet Manifold Stress, Line and Shock Loads

2. First-Stage and Second-Stage Rotors

a. First-Stage Rotor Stress

The final rotor configuration was the result of a stress analysis program wherein an initial design was analyzed, revised, and re-analyzed. This process was repeated until an optimum configuration was developed. The optimum configuration yielding a turbine which is of minimum weight while structurally adequate.

The stress analysis considered the following stress producing items: centrifugal; pressure; thermal; vibration; and thermal fatigue.

The first step in the analysis was to determine the critical time period in terms of maximum thermal stresses. This was found to be 230 sec from the time equal to zero in the pump start and operation cycle. The results of the analysis show the following:

(1) Local yielding will occur in the turbine rotor bore as a result of the combined centrifugal and thermal stresses. The maximum theoretical stress level is 275,000 psi at 230 sec running time. This stress level occurs in a local area of the 1.875-in. diameter bore through the turbine disc. Table No. I gives a tabulation of the disc bore stress from 10 sec to 230 sec.

TABLE I

FIRST STAGE DISC STRESS

| CONDITION (SEC) | *MAX. TANG. STRESS (KSI) | LOCATION | YIELD (KSI) | ULTIMATE (KSI) | ELONGATION % |
|---|---|---|---|---|---|
| 10 | 150 Ten. | Bore | 165 | 230 | 15 |
| 60 | 240 Ten. | Bore | 165 | 230 | 15 |
| 100 | 220 Ten. | Bore | 165 | 230 | 15 |
| 120 | 265 Ten. | Bore | 165 | 230 | 15 |
| 230 | 275 Ten. | Bore | 165 | 230 | 15 |

*The average tangential stress is 65 KSI at 14,550 rpm.

(2) The theoretical local stress value (calculated elastic stress) is not considered to be detrimental since it is less than twice

the material yield stress value[5].

During the first stress cycle, local plastic flow will occur but in subsequent cycles all local deformation will be elastic. When cycling is purely elastic, the low-cycle, plastic strain fatigue failures are not probable.

(3) Burst speed is 21,800 rpm.

(4) Margin of safety, which includes a safety factor of 1.5, is +0.49 based upon an average stress of 65,000 psi.

The rotor blades were treated in a separate analysis. The stress analysis included centrifugal forces, pressure load, thermal effects, vibration, and thermal fatigue. The alternating stress was assumed to be 30% of mean stress. The blades were shown to be adequate in all respects (see Figure No. 20). The margin of safety is +.72 at 1300°F based upon a maximum stress of 59,000 psi which includes a safety factor of 1.2. The highest thermal stress in the blade occurs 1.25 sec after start (see Figure No. 21) and is calculated to momentarily reach 110,000 psi.

The turbine shaft stress analysis was a case of proving the spline to be adequate. The basic assumption was that only 25% of the spline teeth were engaged and carrying the full torque. The shaft is adequate because calculations give the following margins of safety:

Cycle bending = 0.62 based on a modified Goodman diagram and stress of 63,800 psi which includes a safety factor of 1.25. The cyclic bending stress includes the effect of an assumed alternating stress of 10% of the static stress plus a stress concentration factor of 1.505 applied to the cyclic stress.

Cyclic shear = +0.18 based on a modified Goodman diagram, and a stress of 52,500 psi which includes a safety factor of 1.25. The cyclic shear stress includes an assumed alternating stress of 10% of the static stress plus a stress concentration factor of 1.505 applied to the cyclic stress.

Compression = +.30 based upon a stress of 90,500 psi which includes a safety factor of 1.1.

The shaft stress values are conservative because only the room temperature material mechanical properties were used. The cryogenic

---

[5] Criteria from Section III of the ASME Boiler and Pressure Vessel Code for Nuclear Vessels, p.6, Library of Congress, Catalog Card No. 56-3934, 1963

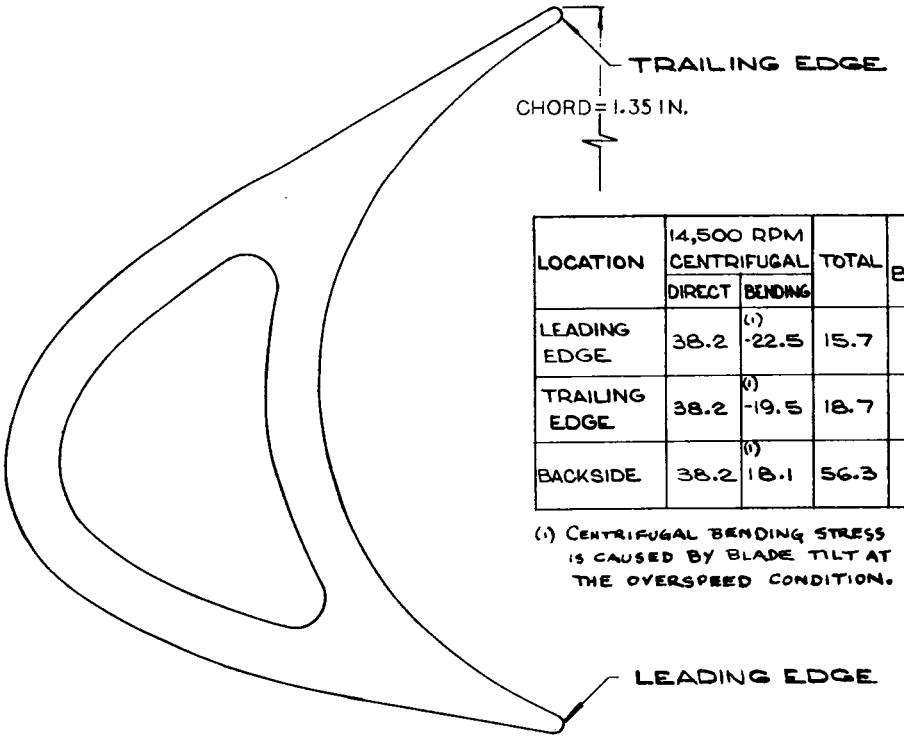


| LOCATION | 14,500 RPM CENTRIFUGAL | | TOTAL | GAS BENDING | TRANSIENT THERMAL | TRANSIENT TOTAL | STEADY TEMP TOTAL | MARGIN OF SAFETY | |
|---|---|---|---|---|---|---|---|---|---|
| | DIRECT | BENDING | | | | | | YIELD | RUPTURE |
| LEADING EDGE | 38.2 | (1) -22.5 | 15.7 | 10.2 | -107.6 | 81.7 | 25.9 | +.72 | +.52 |
| TRAILING EDGE | 38.2 | (1) -19.5 | 18.7 | 5.7 | -107.6 | -83.2 | 24.4 | | |
| BACKSIDE | 38.2 | (1) 18.1 | 56.3 | -7.0 | -97.6 | -48.3 | 49.3 | | |

(1) CENTRIFUGAL BENDING STRESS IS CAUSED BY BLADE TILT AT THE OVERSPEED CONDITION.

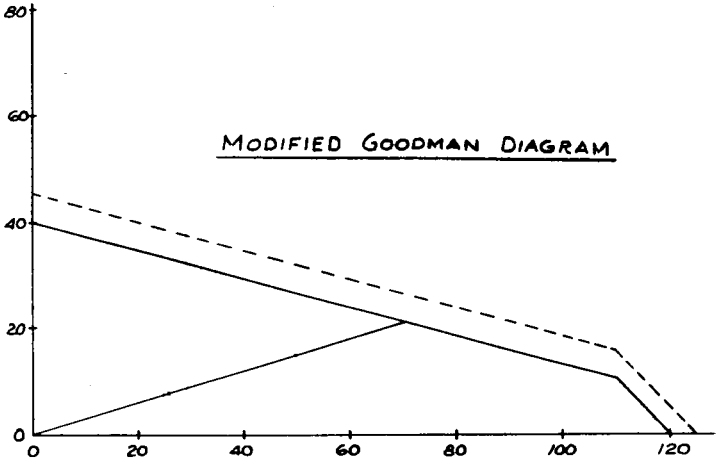


Figure 20

First-Stage Blade Stress

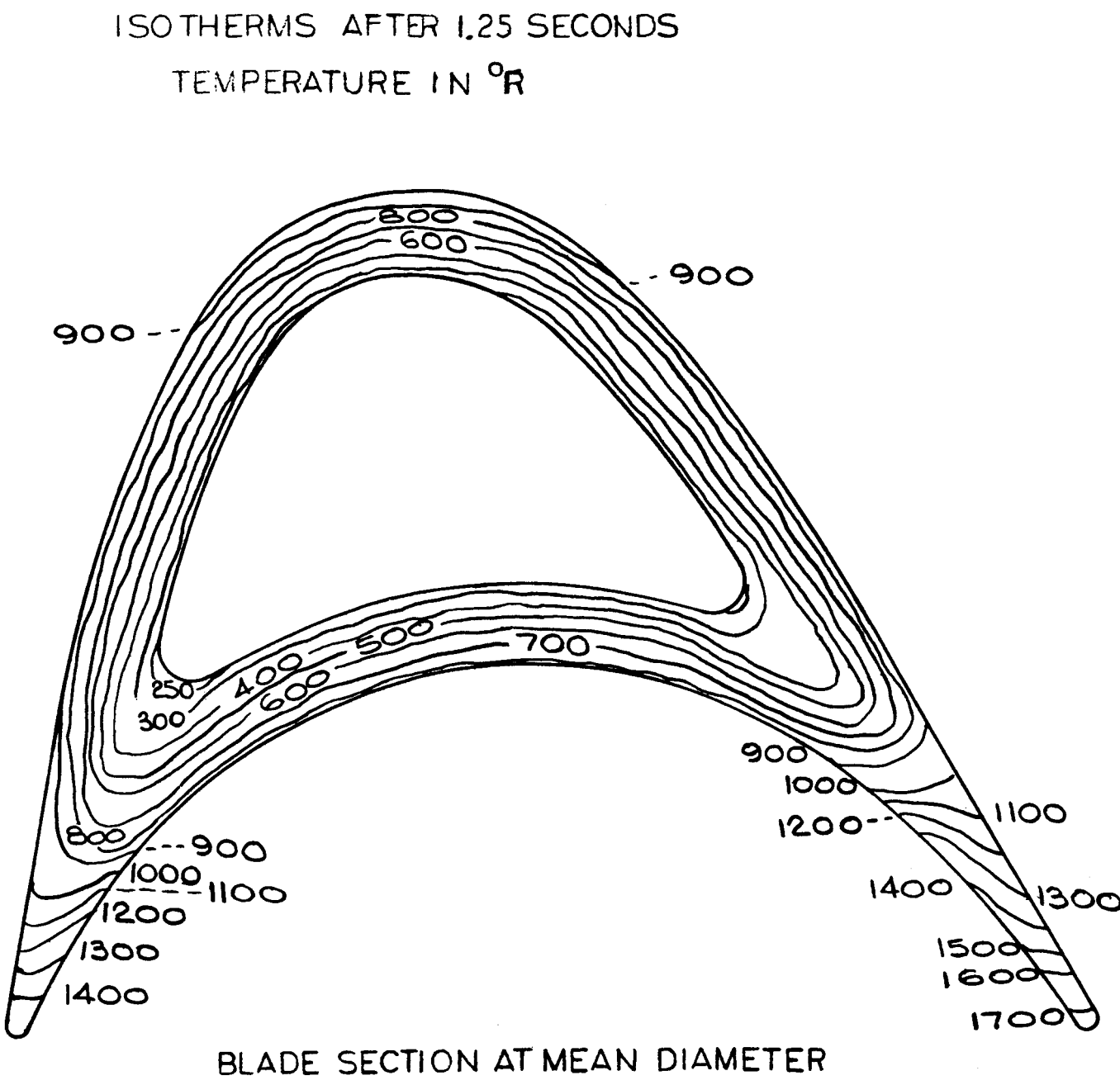


Figure 21

First-Stage Blade Temperature Gradients

mechanical properties as well as the ultimate tensile and yield stresses are considerably higher.

b. First-Stage Rotor Vibration

Calculated values for resonant points of the blades revealed no problem areas. The resonant speeds associated with the first harmonic of the 37 nozzles passing frequency and exciting the first axial and tangential bending modes of the blades are as follows:

Tangential = 10,400 rpm

Axial = 11,600 rpm

The blades are considered adequate because these vibration values are sufficiently removed from the pump design operating point so as to cause no problem. These frequencies will be passed through quickly during the start transient and shutdown phases of pump operation. Figure No. 22 shows all of the blade vibration frequencies. The primary stimuli are the 37 nozzles upstream of the blades.

The turbine disc was analyzed with respect to axial vibrations. Preliminary calculations revealed that the two nodal diameter mode shapes gave the lowest critical speed values. Assumed values of radial and tangential stress representative of expected stress were used in this analysis to obtain the minimum critical speeds. The results are as follows:

Static = 14,370 rpm for a radial stress of 100,000 psi and a tangential stress of 50,000 psi.

10% overspeed = 18,000 rpm.

These critical speed values, when compared with the pump operating speed range, show the turbine disc design to be satisfactory.

c. Second-Stage Rotor Stress

The stress analysis for this turbine rotor was made concurrently with the first-stage turbine rotor. All criteria were the same and included centrifugal forces, pressure load, thermal effects, vibration, and thermal fatigue. Alternating stress was assumed to be 30% of the mean stress.

The final design is the result of repeated analyses wherein disc profiles were altered as problem areas or lightly-stressed areas were uncovered. The final configuration is considered optimum. The following are the calculated values from the final analysis.

Burst speed is 22,100 rpm.

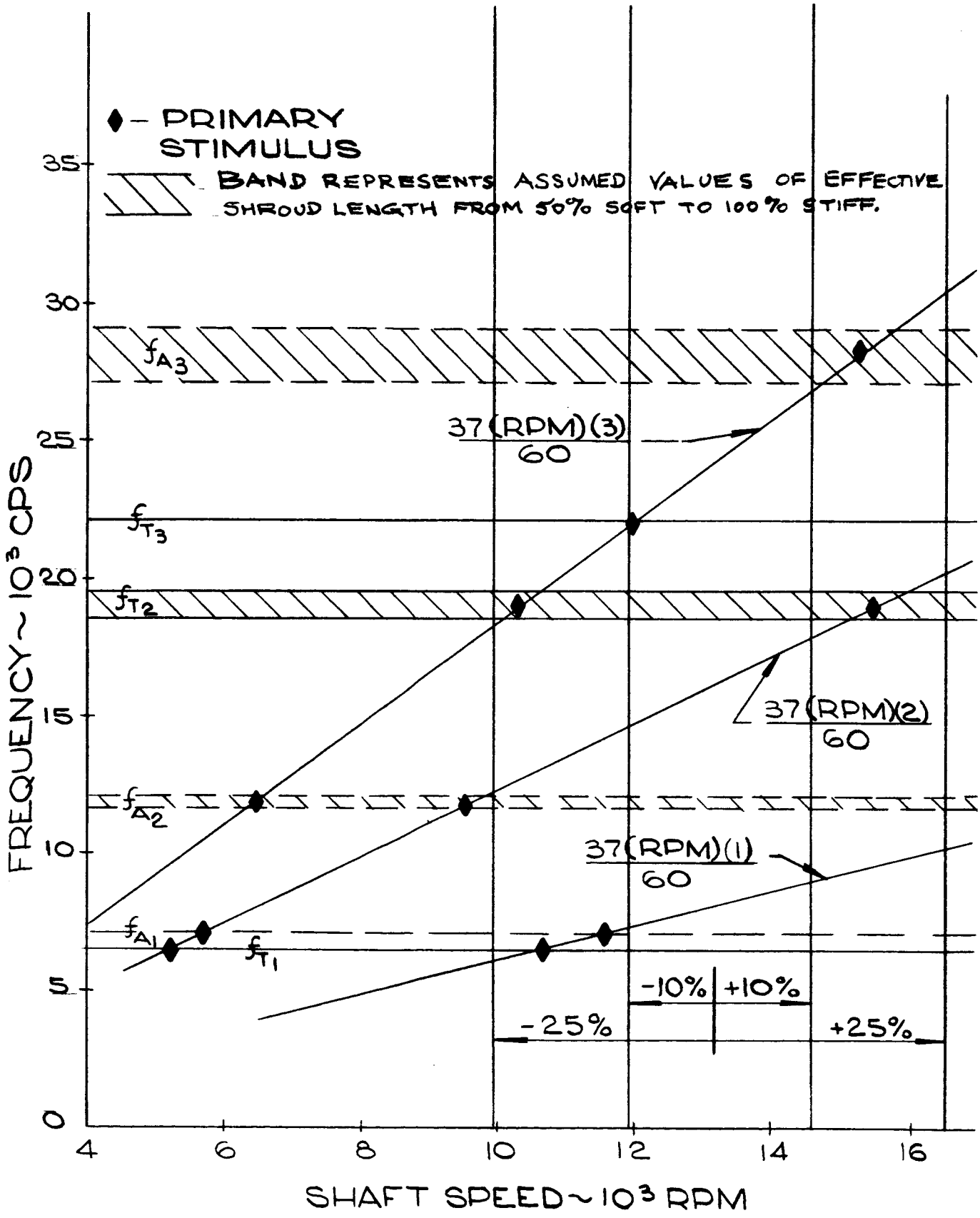


Figure 22

First-Stage Blade Vibration Frequencies

The margin of safety, which includes a factor of safety of 1.5, is +0.53 based upon an average tangential stress of 66,000 psi. Figure No. 23 shows a tabulation of the disc stresses, which include thermal stresses.

A maximum combined theoretical stress of 205,000 psi occurs in the local area on the surface of the 1.562-in. diameter bore through the center of the turbine disc. This stress level is not considered detrimental because it is less than twice the yield stress value for the material.

The curvic coupling stress values proved to be relatively low. The maximum stress is 55,600 psi. The minimum margin of safety is +0.37 including a safety factor of 1.2.

The blade stress analysis yielded the following results:

(1) Maximum combined stress of 61,440 psi.

(2) Margin of safety to yield point at 1300°F is +.38, including a safety factor of 1.2.

(3) Margin of safety to rupture is +.22 including a safety factor of 1.6.

Figure No. 24 summarizes the blades stresses.

The blades are considered satisfactory in all respects.

d. Second-Stage Rotor Vibration

The vibration analysis was made using the same criteria as used for the first-stage turbine rotor. The primary stimuli are the 67 upstream reversing vanes. Secondary stimuli are the 37 nozzles upstream of the first rotor. The calculated resonant frequencies for the blades expressed in terms of pump revolutions per minute are as follows:

First tangential = 1100

First axial = 2100

First torsional = 3100

Second tangential = 10,100

Second axial = 14,900

Second torsional = 12,100

$\sigma_R$ - RADIAL STRESS

$\sigma_T$ - TANGENTIAL STRESS

$F_{ty}$ - TENSILE YIELD STRENGTH OF MATERIAL

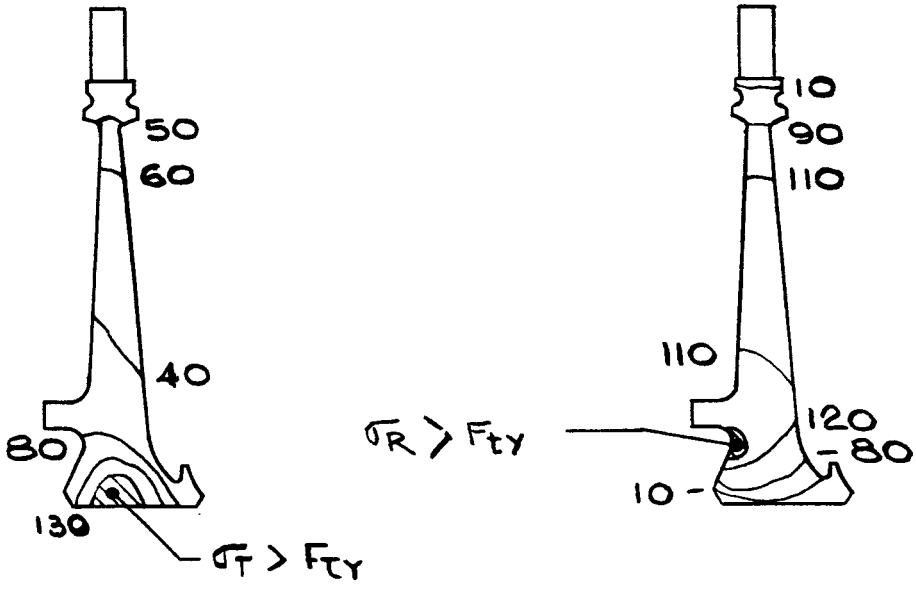


TANGENTIAL COMBINED

RADIAL COMBINED

| | MAX STRESS (KSI) | TYPE STRESS | TEMP | ALLOWABLE STRESS (KSI) |
|---|---|---|---|---|
| CENTRIFUGAL 14,550 RPM | 90.0 | TANG. | 660°F | 130 |
| | 110.0 | RADIAL | 665°F | 130 |
| THERMAL 100 SEC | 110.0 | TANG | -60°F | 150 |
| | 85.0 | RADIAL | -60°F | 150 |
| COMBINED | 205.0 | TANG | -60°F | 150 |
| | 155.0 | RADIAL | -60°F | 150 |

AVERAGE $\sigma_T$ = 66 KSI AT 14,550 RPM

Figure 23

Second-Stage Disc Stress

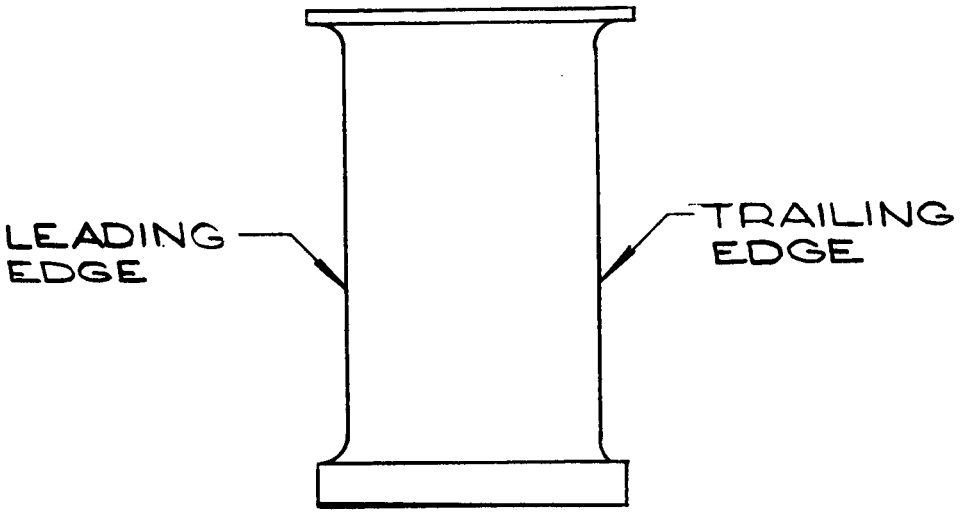


| LOCATION | 14,550 RPM CENTRIFUGAL | | TOTAL | GAS BENDING | STEADY TEMP TOTAL | MARGIN OF SAFETY | |
|---|---|---|---|---|---|---|---|
| | DIRECT | BENDING* | | | | YIELD | RUPTURE |
| LEADING EDGE | 56.8 | -11.7 | 45.1 | 8.0 | 53.1 | .38 | .22 |
| TRAILING EDGE | 56.8 | -11.4 | 45.4 | 8.0 | 53.4 | | |
| BACKSIDE | 56.8 | 11.4 | 68.2 | -6.8 | 61.4 | | |

THERMAL STRESSES NOT CALCULATED FOR THIS BLADE AND ARE NOT SIGNIFICANT

*CENTRIFUGAL BENDING STRESS IS CAUSED BY BLADE TILT AT OVERSPEED CONDITION.

Figure 24

Second-Stage Blade Stress

These resonant frequencies present no problem when compared with the pump operating speed band. Figure No. 25 shows a plot of the various vibration frequencies.

The turbine disc axial vibration was analyzed. As in the case of the first stage turbine, only the two nodal diameter modes were investigated because this provided the lowest critical speed values. This analysis revealed the following:

(1) Static critical speed is 14,430 rpm with 100,000 psi radial and 50,000 psi tangential loads.

(2) At 14,550 rpm, the disc axial critical speed is 17,640 rpm with 100,000 psi radial and 50,000 psi tangential loads.

These critical speeds are satisfactory when compared with the pump design operating speeds.

3. Reversing Row

a. Stress

Stress analysis of the reversing vane segments considers loads resulting from gas pressure and velocity. The thermal-induced loads were made negligible by design of the component. The analysis shows the minimum margin of safety to be +1.7 and the maximum stress to be 27,400 psi. The stresses are tabulated in Figure No. 26.

b. Vibration

Vibration analysis of the reversing vanes shows the highest resonant frequency, expressed in terms of pump speed, to be the third tangential mode at 10,000 rpm. All other modes are below this frequency. When compared with the pump operating speed band, the reversing vanes present no difficulty as pertains to vibration. Figure No. 27 shows all of the vibration frequencies.

4. Rotor Tie-Bolt

To prevent joint separation during all conditions of thermal and dynamic loading, a bolt pretorque of 11,500 in.-lb is required (see Figure No. 28). With this pretorque, and during the worst period of thermal gradients, the margin of safety is +0.19. This includes stress concentration factors up to 2.78, a factor of safety of 1.2, and a thread coefficient of friction of 0.15.

The natural frequency of the tie-bolt, with the center piloted, occurs at 52,500 rpm. This is well above the operating speed.

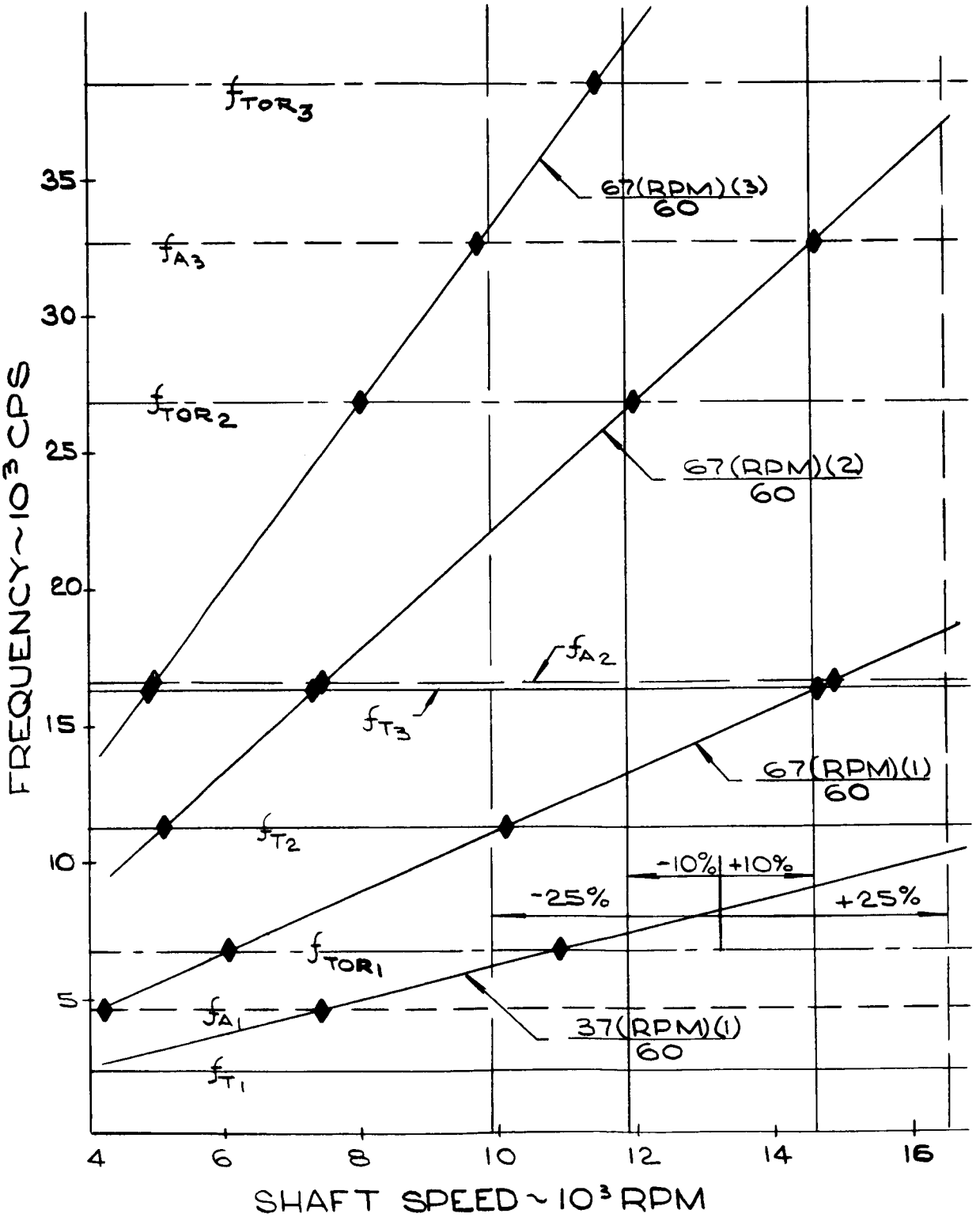


Figure 25

Second-Stage Blade Vibration Frequencies

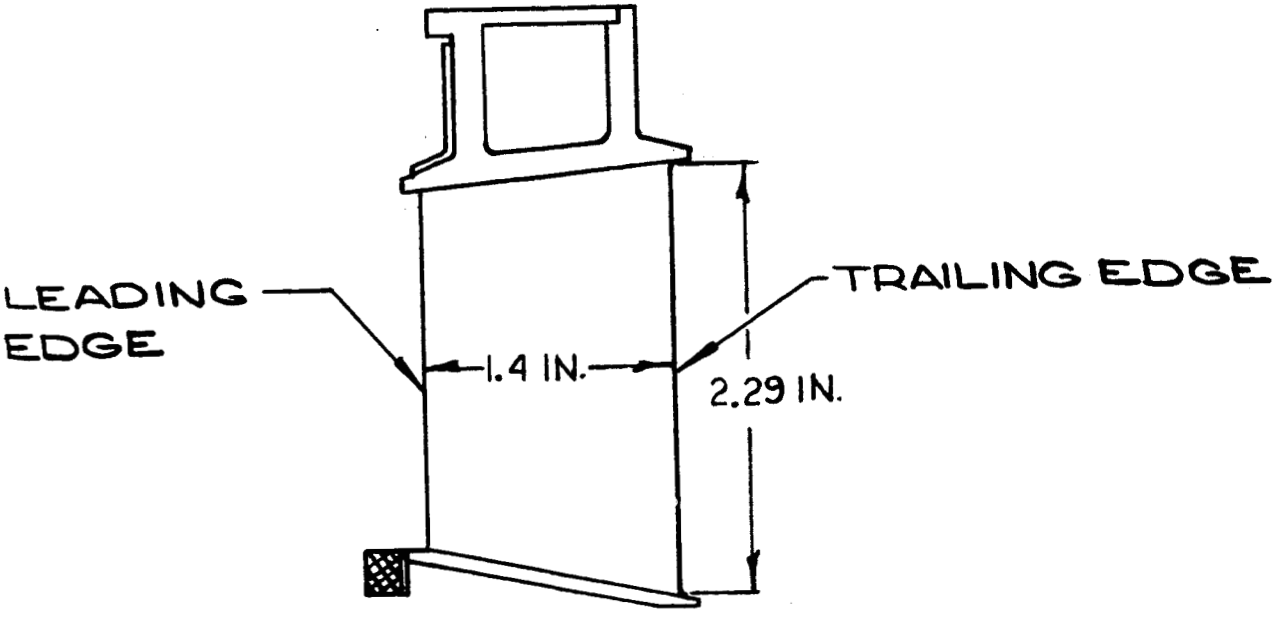


| LOCATION | GAS BENDING | TRANSIENT THERMAL | STEADY TEMP. TOTAL | MARGIN OF SAFETY | |
|---|---|---|---|---|---|
| | | | | YIELD | RUPTURE |
| LEADING EDGE | 25.9 | * | 25.9 | +2.0 | +1.7 |
| TRAILING EDGE | 22.4 | * | 22.4 | | |
| BACKSIDE | -27.7 | * | -27.7 | | |

* THERMAL TRANSIENT STRESSES INSIGNIFICANT

Figure 26

Reversing Row Stress

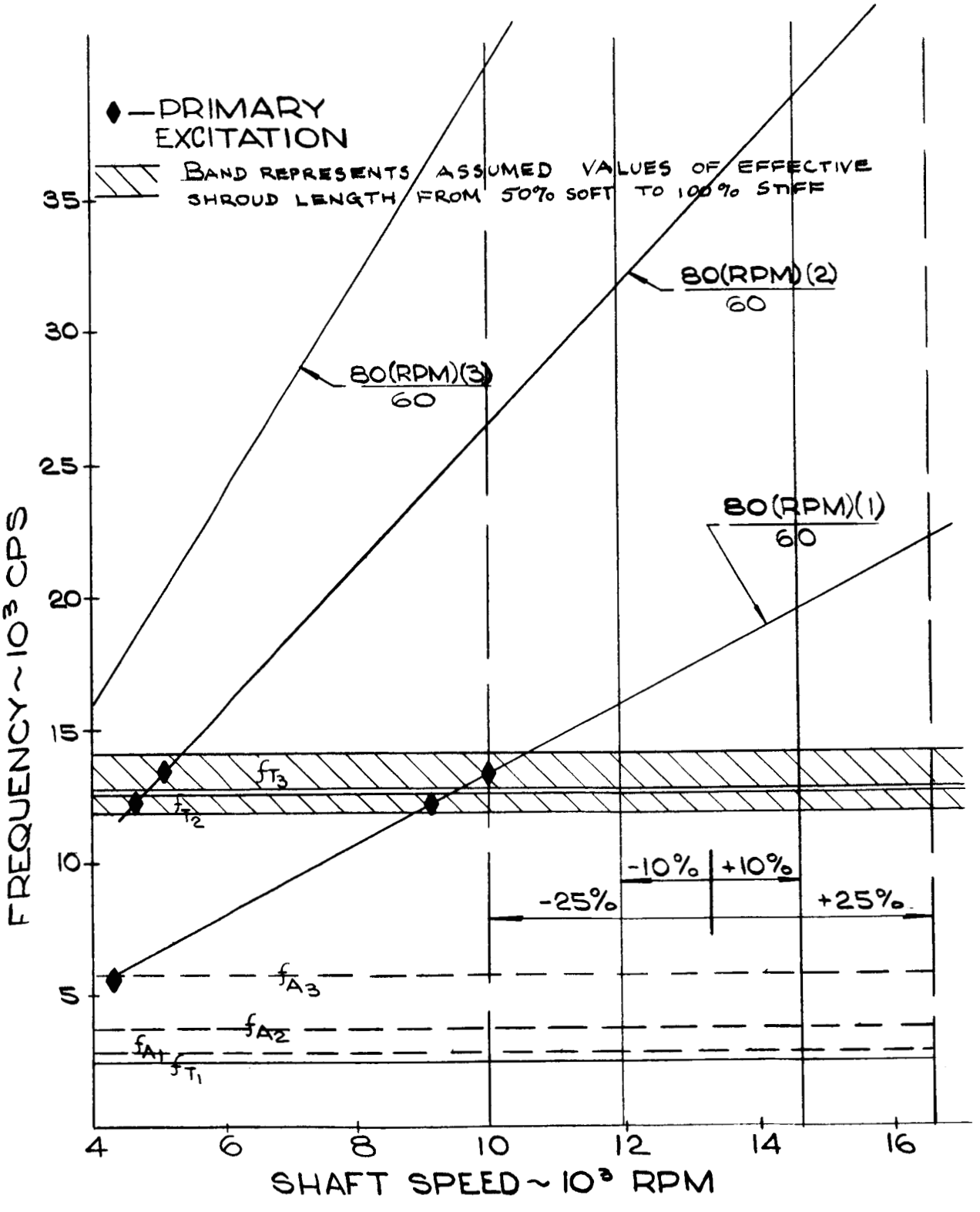


Figure 27

Reversing Row Vibration Frequencies

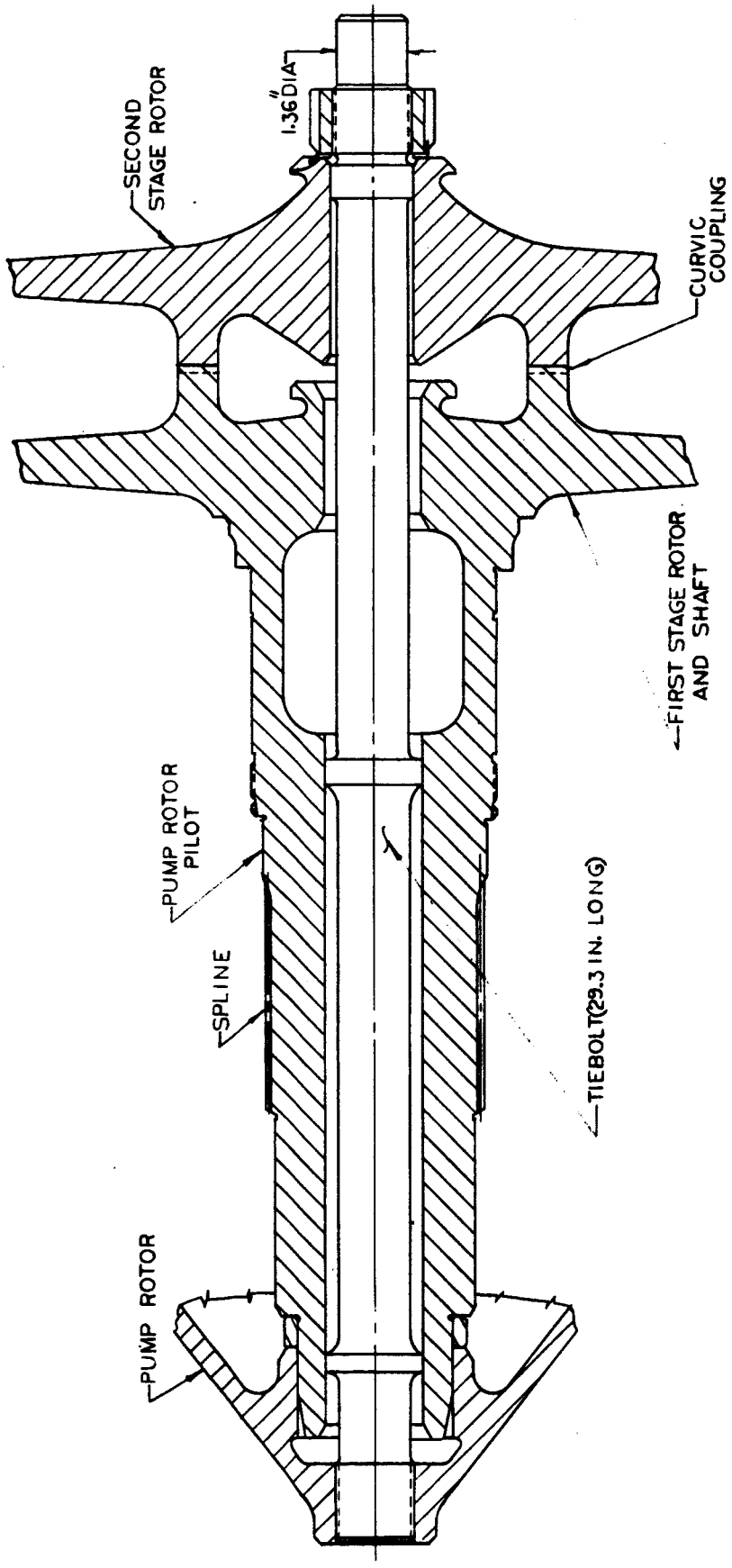


Figure 28

Turbine Rotor, Tie-Bolt and Adjacent Parts

5. Bearing Housing Seal

The most severe stress, pressure, and thermal gradients contained in the seal components, plus the thermal movements of the inlet manifold, were considered.

The most severe stress occurs 10 sec after start-up at the junction with the end of the bellows and the inner support cone (see Figure No. 29). This stress is caused by bending. The apparent computed elastic stress is 443,000 psi. Yielding will occur and the problem becomes one of low cyclic fatigue because the primary membrane stress is low.

A low cyclic fatigue analysis of the bellows revealed failure will occur after 520 cycles. However, when a factor of safety of 1.6 is applied to the total strain, the fatigue limit reduces to 222 cycles. A cycle is described as a hot gas run of at least 10 sec.

6. Turbine Exhaust Housings

Two different exhaust housings are used on the M-1 fuel turbine. An exhaust cone frustum is used when the turbopump is tested apart from the engine. For complete engine tests, a dual exit hemisphere exhaust housing is used.

a. The Exhaust Cone (Figure No. 13)

The structural evaluation of the exhaust cone is based upon the following extreme operating conditions at the test stand.

(1) Gas temperature - 1025°F

(2) Maximum Internal Pressure - 386 psia

(3) External applied loads - 400,000 in-lbs bending moment.

The margin of safety, based upon the ultimate strength of the material at 1025°F, with a 1.6 factor of safety, is 1.17 for hoop stress and 4.5 in buckling from the bending moment.

b. Dual Exit Exhaust Housing (Figure No. 14)

The stress analysis for the turbine exhaust housing includes the following loads:

(1) Internal Pressure

(2) Inertial-induced line loads on the cross-over duct

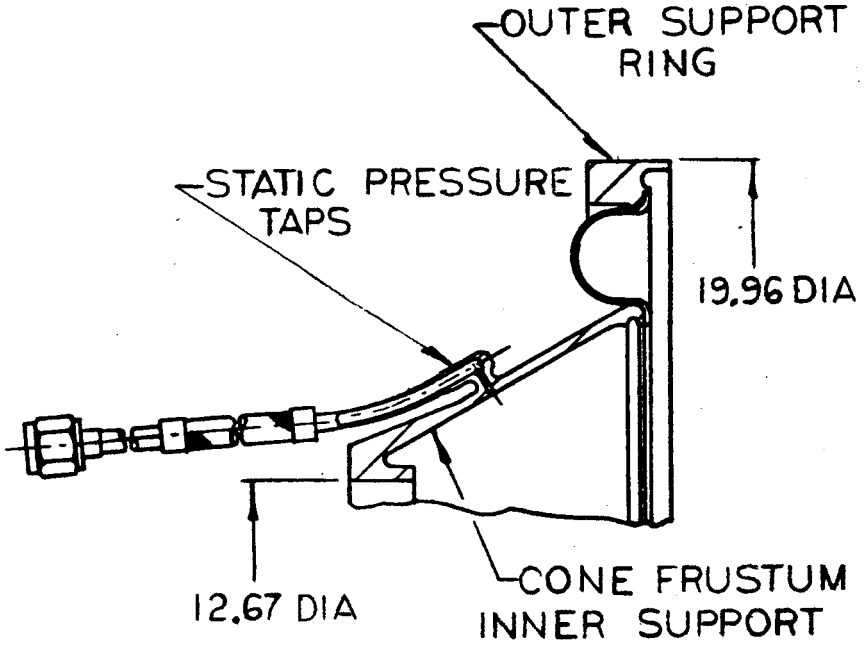


Figure 29

Bearing Housing Seal Assembly

flanges and on the propellant utilization valve flange.

(3) Vibration-induced line loads at all flanges.

The material strength at 1000°F was used to determine margins of safety. Thermal-induced stresses were not determined. They were considered to be minor because of the thin walls and the type of construction, which does not restrain the housing.

The factor of safety for pressure loading is a factor of 1.6 based upon an ultimate strength of 155,000 psi at 1000°F.

The factor of safety for inertia loading is a factor of 1.5 based upon an ultimate strength of 155,000 psi at 1000°F.

The maximum combined stress occurred in the spherical-shaped wall at a point approximately midway between the propellant utilization valve flange and the junction of the transition to the 11.4-in. diameter cross-over flange. The minimum margin of safety at this point was calculated to be +0.17.

7. Support Frame and Turbine Main-Flange Clamps (Figures No. 2 and No. 9)

The stress analysis was performed to determine the structural integrity of the frame with loads as imposed at the test stand. These loads include the test area turbine exhaust adapter line and its bellows. It was assumed that the bellows would have a spring rate of 4500 lb/in. in the axial and transverse directions and would deflect one inch in each direction during operation. The maximum expected pressure in the manifold is 1175 psi and in the exhaust cone, 386 psi. The maximum expected temperature is 1300°F.

With these conditions, the margin of safety, based upon the material yield strength with a 1.0 factor of safety, is 1.09 and based upon the ultimate strength with 1.5 factor of safety, the margin of safety is 0.97. The bolts attaching the frame to the pump discharge housing (AS4013, P/N 712329-311) have a margin of safety of 0.60 based upon the yield strength and 0.18 based upon ultimate strength.

The bolts attaching the half-clamps to the frame ends and the paired clamps, have a margin of safety based upon yield strength of 0.36, with a bolt pretorque of 1190 in.-lb.

The main flange joint margin of safety, with a factor of safety of 1.6 based upon the material ultimate strength, is 0.28.

## F. DYNAMIC BALANCING AND ASSEMBLY TECHNIQUES

### 1. Dynamic Balancing

The dynamic balancing of the turbine rotors is accomplished in a series of steps, starting with the first-stage turbine and ending with the complete turbopump rotating assembly. All balancing is performed on a Gisholt U type machine. The engineering dynamic balance requirements are based upon limits that can be readily achieved with the U type machine. The balancing sequence is as follows:

a. The first-stage turbine rotor is balanced using a two plane system.

b. The second-stage turbine rotor is installed on the balanced first-stage turbine rotor and the assembly is checked for the degree of unbalance. The second-stage rotor is removed and rotated relative to its initial position. It is then reassembled to the first-stage rotor. The amount of unbalance is again determined. This sequence is repeated as often as necessary to ascertain the assembled condition that provides the least unbalance. The assembly is then balanced to the drawing requirements with corrections made to the second-stage only. The rotors are match-marked.

c. The balanced turbine rotor assembly is installed in a balanced pump rotor assembly. The condition of least unbalance is determined by repeated disassembly, rotation, and reassembly. The complete rotating assembly, having the smallest degree of unbalance, is balanced using a two plane system. All components: pump rotor, first-stage turbine rotor, second-stage turbine rotor, and tie-bolt are match-marked and identified with a common serial number.

### 2. Assembly Techniques

The turbine components are assembled to the fuel pump in the following sequence (use Figure No. 2 as a reference).

a. The turbine frame is bolted to the pump discharge housing.

b. The turbine inlet manifold is attached to the turbine frame by means of an assembly fixture.

c. A gaging tool, which simulates the turbine shaft and disc, is installed in the pump rotor. Measurements are made from gaging surfaces on the tool to various surfaces on the inlet manifold and turbine bearing housing. These measurements are recorded and the gaging tool is removed.

d. The recorded measurements are used to calculate the following:

(1) The shim thickness required at the turbine frame discharge housing interface to correctly position the turbine inlet manifold, relative to the turbine bearing housing.

(2) The spacer length required to correctly position the first-stage turbine relative to the turbine bearing housing for proper lift-off seal operation.

e. The turbine frame shims are installed in the turbine frame discharge housing interface and the bolts are torqued.

f. The inlet manifold position is checked relative to the turbine bearing housing. The diaphragm seal, which forms the closure between the inlet manifold and the turbine bearing housing, is installed and the gas tungsten arc welds are made.

g. The first-stage turbine rotor is installed as follows:

(1) Warm gaseous nitrogen is flowed through the turbine bearing housing to raise the temperature of the pump rotor.

(2) The turbine shaft is placed in liquid nitrogen.

(3) When the temperatures of the components become stabilized, the first-stage rotor is positioned by aligning spline teeth and dynamic balancing match marks, then inserted into the pump rotor. This operation is completed as rapidly as possible.

(4) The turbine tie-bolt is installed with suitable fixtures to permit applying an axial load to the turbine equivalent to the final assembly preload. The assembly is allowed to return to room temperature.

(5) The reversing row is installed with the anti-rotation slots aligned with the lugs in the inlet manifold main flange.

(6) The fixture is removed from the turbine bie-bolt. The second-stage rotor is installed, taking care to align curvic coupling teeth and dynamic balancing match marks.

(7) The turbine tie-bolt is positioned axially. The nut and lock ring are installed and torqued to drawing requirements.

(8) The fixture, which has been positioning the inlet manifold, is removed and the exhaust housing is installed. The exhaust housing is held in position with a minimum number of clamps to provide access to the flange for welding. The turbine inlet manifold and exhaust housing joint is sealed by gas tungsten arc welding. After the welding is completed and leak

checks are made, all clamps are installed and torqued to drawing requirements.

(9) The assembly is completed by adding appropriate closures as required to protect the unit.

## G. DESCRIPTION OF COMPONENT FABRICATION

### 1. Turbine Inlet Manifold

The turbine inlet manifold is a completely gas tungsten arc welded (GTAW) assembly composed of a torus, nozzle ring, and turbine casing (see Figure No. 10). Inconel 718 alloy[6] is used for all components. Parts are stress relieved after each weld is completed. After the subassemblies are welded into the final assembly, the complete manifold is heat treated by solution-annealing and aging.

The torus is formed from sheet material into doughnut-shaped half-shells. These half-shells are then GTAW welded together on the outside diameter and inside diameter forming a complete doughnut. An eight inch diameter inlet neck is inserted at an eighteen degree angle, using double thickness material for fifteen degrees to each side of the center, which is the reinforced hole cutout area. A conoseal flange with twenty-four bolt holes is welded on the upstream end of the inlet neck for attachment of the helium start line, the hot gas by-pass line, and the emergency blow-off valve.

On the downstream side of the torus, a 4.5-in. wide slot is machined out on a 23.0-in. mean diameter for insertion of the nozzle ring. This nozzle ring has flange extensions that match the torus walls, which facilitate GTAW welding the two parts together.

The nozzle ring is made from two forged rings and thirty-seven forged nozzles, all GTAW welded together. The nozzles are rough-forged into approximate shape in a long section; then, several nozzles are cut from each section. The outside profile is ground to close tolerances and forms the gas passage. The inside of the nozzle is electrical discharge machined to give a wall thickness of 0.125-in. This reduces thermal stresses and allows the low pressure gas to circulate between the outside diameter and inside diameter giving better pressure distribution and more even thermal gradients.

A turbine casing, which contains the main flange is then welded to an extension on the outer ring, completing the nozzle ring assembly (see Figures No. 10 and No. 11).

---

(6) Frick, V., Hunt, V., Inouye, F. T., and Janser, G. R., Summary of Experience Using Inconel 718 on M-1 Engine, Aerojet-General Report No. 8800-37, 1 March 1966 (To be published as a NASA Contractor Report)

The torus downstream diameters are now carefully machined to match the nozzle ring extensions and the two parts are fastened together by circumferential welds. These welds are penetrant inspected as well as radiographically inspected. The part is then heat-treated, proof tested, and leak tested. The last process is to finish machine all flanges and indexing surfaces.

Some welding problems were experienced with the 718 alloy. The main problem was from contamination, (i.e., occlusions in the weld rod, impurities in the helium and argon gas shields, dust contaminated weld booths, and improper gas shielding of the weld). Weld shrinkage and warping, which is not restricted to 718 alloy, was also a problem. Proper fixturing and improved welding procedures eliminated the latter problem. Optimum weld joint configuration caused some concern and required the use of sample weld joints to arrive at the best solution.

2. First-Stage Rotor and Blades

The turbine rotor is characterized by a shaft extending from one side of the turbine disc. This shaft is installed into the pump rotor forming a rigid joint for the transmission of power. The turbine shaft has a spline and two piloting diameter, which form the interface to the pump rotor. The turbine shaft also carries the journal for the turbine end roller bearing. Figure No. 3 shows a cross-section of the rotor, shaft, and blades.

The turbine disc side opposite from the shaft has a curvic coupling (see Figure No. 5). This coupling serves as both the power transmission and locating device for the second-stage turbine rotor.

The turbine disc is of minimum thickness consistent with structural integrity. The disc contour was derived from an elaborate stress analysis which included not only all operating loads but also all thermal stresses generated during chilldown and start transient phases. The final disc shape represents the optimum configuration which satisfies both functional and weight criteria.

The periphery of the turbine disc has 80 blades. Each blade has an integral tip shroud for increased performance. As a result of vibration analysis, the blade shrouds are joined by welding at 40 places, the alternate shroud joints being the ones welded. The blades are hollow to reduce weight, which, in turn, reduces rotational loads imposed upon the turbine disc. The blades are attached to the turbine disc by electron-beam welding. This method of fabrication produces the minimum weld area, which, in turn, results in the minimum disc rim size to accept the blades.

a. Machining Process Techniques

The blades were machined from Inconel 718 die forgings.

The machining process used several different techniques.

(1) The concave airfoil surface was made by electro-chemical milling, ECM. This uses an electrode which duplicates the desired shape. Material is removed passing electric current from the electrode through a conductive salt solution to the metal being worked. No spark is involved.

(2) The remaining airfoil surfaces and shroud contours were made by conventional blade milling operations.

(3) The blade platform and shroud platform configurations were machined by electro-chemical grinding, ECG.

(4) Blade cavities were produced by the ECM process.

Each blade was completed by welding a cap into the end of the cavity. This cap was necessary for adequate shroud strength.

The turbine shaft is made from a Rene' 41 forging, which was selected not only for its strength, but also for its coefficient of thermal contraction, which is smaller than Inconel 718. This difference in thermal contraction permits the Rene' 41 shaft to have a slightly loose fit (at room temperature) into the Inconel 718 pump rotor, yet have an interference fit at pump operating temperature. This feature makes assembly less difficult and produces a rigid joint at cryogenic temperatures, which is essential for satisfactory power transmission as well as for maintaining the close running clearances within the pump.

The turbine disc is manufactured from an Inconel 718 forging. This material provides both the high strength required and the necessary ductility at both cryogenic and elevated temperatures. This material is capable of accepting the large thermal gradients involved during the pump start cycle.

As mentioned previously, the turbine components are joined by electron-beam welding. This method provides a very narrow weld and heat affected zone with mechanical properties equal, or nearly equal, to the parent material. The narrow weld and the necessary metal-to-metal fit of the parts being joined make possible a joint configuration, which requires the least mass of material, thus producing a part of minimum weight.

All welds are inspected by dye penetrant, radiographic, and ultrasonic methods. The welds were made with a minimum of difficulty. Some defects did occur because of the electron-beam passing out of the joint, but these defects were removed in subsequent machining operations, leaving a weld of high quality.

All machining other than that mentioned above was accomplished by conventional methods.

b. Manufacturing Problem Area

Only one real problem was encountered during manufacturing. This was the welding of the cap which closes the blade cavity. Initial welding resulted in poor weld penetration and cracked blades. Aerojet-General Welding Engineers found the problem was caused by:

(1) Too much heat was used during the welding.

(2) The surfaces to be joined were not adequately cleaned.

(3) Poor weld technique was used in method of weld application as well as the sequence of operation.

(4) The welding equipment was in need of repair.

The necessary corrective actions were undertaken by the Aerojet-General Corporation Welding Engineers and they also supervised the actual welding of the caps into each blade. The welding proceeded satisfactorily under these conditions.

No other problem areas were encountered. Electron-beam welding proved to be trouble-free. Full-scale sample welds were made prior to joining the actual turbine components. Weld joint preparation, as regards fit and surface finish, was established from the weld joint samples.

3. Second-Stage Rotor and Blades

The second-stage turbine rotor is essentially a disc having 78 blades on its circumference (see Figures No. 6 through No. 8). The blades have a tip shroud, which is segmented in that each blade has a section of the shroud as an integral piece. The shroud segments are not joined between blades as on the first-stage turbine. Figure No. 6 shows a cross-section of the disc and the blade profile.

The blades are reduced in weight by means of an internal cavity, machined from the blade tip inward. This cavity is covered with a thin cap that is welded into place. Blades are machined as individual items from Inconel 718 die forgings.

The turbine disc is machined from an Inconel 718 forging. The disc cross-sectional shape is the direct result of stress analysis aimed at producing a part of minimum weight. One side of the disc has a curvic coupling, which serves as the interface to the first-stage turbine rotor. The coupling not only positions the turbine rotor properly, but also transmits the power developed. The opposite side of the turbine has a hub contour, which has a suitable face for the turbine tie-bolt installation and a grooved area to aid in disassembly.

4. Reversing Vanes

The reversing vane row is comprised of six segments. There are five segments having 11 vanes each and one segment having 12 vanes for a total of 67 vanes per row. Each segment is a welded assembly made up of an inner shroud, vanes, and an outer shroud. The inner shroud is divided so that there are two blades per shroud segment. The slot forming this division is stepped so as to interlock the adjacent blades. These slots are required to minimize the thermal stresses resulting from the expansion of the segments. A honeycomb seal is installed on the leading edge of the inner shroud between the first-stage turbine rotor and the reversing row to reduce gas leakage to a minimum. Figure No. 12 shows a cross-section through one segment as well as the vane profile and interlocking inner shroud.

The vanes are formed sheet metal units for minimum weight.

The outer shroud segment is a hollow continuous member. A key slot is provided for anti-rotation. The vane segment is mounted in the turbine housing by means of the outer shroud. Where necessary, sheet metal cover-plates are used to prevent gas flow through areas other than the vane passages.

The reversing vane segments were fabricated as a complete ring. The ring was cut apart to form the required six segments. This fabrication method simplified the machining, tooling, and alignment of the many parts required in the weld assembly.

The outer shroud was machined from an Inconel 718 ring forging. Machining the part as a ring made it possible to achieve the tolerances required to make the end product dimensionally acceptable.

The airfoil-shaped holes required to accept the vane ends were machined on the inner diameter of the shroud by electrical discharge machining, EDM.

The vanes were formed from Inconel 718 sheet metal. The overlap and weld joint were made at the trailing edge of the vane. The final airfoil surface was completed by machining the weld deposited material to the desired contour. The inner shroud was formed into a complete ring using Inconel 718 sheet stock as the basic material. The holes required to accept the vane ends were pierced by the EDM method.

The two shrouds were fixtured, the vanes inserted, and the unit welded. Then, the assembly was heat-treated to the full-aged condition. After completing all remaining machining work, the ring was cut into six segments by EDM. The EDM electrodes do not actually touch the work piece; therefore, it was possible to use a very thin electrode to produce the shroud slots and segments from a single ring assembly.

Excessive distortion occurred when the first full ring was cut into the six vane segments. Investigation revealed that this distortion resulted from the heat-treating operation. The ring weld assembly had not been restrained in a fixture during the heat treat cycle. A fixture was constructed and used for the second weld assembly. The vane segments cut from the second unit exhibited some distortion, but all parts were acceptable for use.

5. Rotor Tie-Bolt

The function of the tie-bolt is to hold the two turbine rotors securely to the pump rotor. It must withstand the significant thermal movements of the rotating components. In addition, it must hold the forces from the gyroscopic gimbaling loads, the axial acceleration loads, and the curvic coupling separation loads. To accomplish this, a very elastic bolt was required. To obtain this elasticity, the bolt was made as long as possible.

The bolt has a diameter of 1.38-in. and is 29.25-in. long. A 0.5-in. hole is rifle-drilled through the center. The function and positioning of this part is shown in Figure No. 28. The tie-bolt is threaded into the pump rotor at one end. The other end has a nut and lockwasher retaining system, which locates against the second-stage rotor bore extension. To maintain concentricity with the turbine bores and reduce the initial unbalance, piloting shoulders are provided on the tie-bolt at the center and at each end. The center shoulder also damps out the tie-bolt harmonic vibration. The material is Inconel 718 alloy, aged for high strength.

6. Bearing Housing Seal

A flexible closure, between the hot inlet manifold and the cold bearing housing, was required to contain the hot gases in the turbine cavity. The closure had the requirement for accommodating large deflections in both the radial and axial directions and also to retain the hot gas with zero leakage.

The flexible portion of the closure resembles a torus cut in half circumferentially. This was formed from 0.040-in. thick 718 material. It is supported by a stiff ring on the outside diameter and by a cone frustum on the inside diameter. Figure No. 29 shows the bellows and support rings, with a static pressure line attached. Three equally-spaced static pressure taps are provided for performance measurement.

The bellows is spun from 0.040-in. thick sheet into its toroidal shape with extensions protruding for attachment to supporting members.

The outside support ring and the inside support cone frustum are forged from 718 material that is machined to required dimensions. Close toleranced interface surfaces have excess material for removal after welding

and heat treatment.

The three subassemblies are GTAW welded together. The bellows ring is supported axially and radially by the outside diameter and inside diameter support rings; therefore, the GTAW weld is primarily a seal. Flexible hoses and adapters are GTAW welded to the static pressure outlets. The complete assembly is now heat-treated. To determine mechanical integrity, a hydrostatic proof test at 462 psig and a helium leak check at 270 psig are accomplished. Interface dimensions are then finished machined.

7. Exhaust Cone

The exhaust cone is essentially an adapter between the turbine and the test stand exhaust duct. In addition, the large diameter upstream flange mates with the turbine inlet manifold main flange to form the attachment point for the support frame and clamps, which supports the complete turbine assembly. Instrumentation ports are provided for total pressure, static pressure, and total temperature in two axial positions and six tangential positions. Provision is made for orificing the downstream end to control turbine backpressure.

The exhaust cone is a 32 degree cone frustum with flanges at each end. Figure No. 13 shows a cross-section of the cone.

The cone frustum is rolled from 0.125-in. Inco 718 sheet and the seam is GTAW welded. Flanges for each end are rough machined, then GTAW welded to the cone ends. Eighteen instrumentation ports are GTAW welded to the cone surface. All welds are penetrant and radiographically-inspected for quality. The welded assembly is solution-annealed and aged to obtain a combination of stress relief and maximum material strength.

To determine structural integrity, the part is proof tested at 425 psig and leak tested at 200 psig. The final operation consists of finish machining the flanges and indexing surfaces to the final dimensions.

GTAW welding presented some initial problems of gas porosity voids and small cracks in the weld area. This was corrected by improved cleaning, better inert gas coverage, and smaller weld passes with cooling between passes.

8. Dual Exit Exhaust Housing

The dual exit exhaust housing is used when the fuel turbopump assembly operates as part of the complete M-1 engine system. Figure No. 14 shows a cross-section of the exhaust housing and Figure No. 1 shows it assembled with adjacent components.

The exhaust housing is a 26.5-in. diameter hemisphere with a flange on the open end that mates with the turbine inlet manifold main flange.

This forms the attachment point for the support frame and clamps which support the complete turbine assembly. Two 90 degree elbows of 11.4-in. diameter, spaced 120 degrees apart, protrude from the hemisphere-shaped exhaust housing. These elbows provide attachment points for the two cross-over ducts, which carry the exhaust gas and by-pass gas to the oxidizer turbine. The 4.63-in. diameter hot gas by-pass port and gas deflector is placed in the center of the hemispherical end of the exhaust housing.

The exhaust housing shell and protruding elbows are formed from 0.20-in. thick Inconel 718 sheet material. All flanges are machined from Inconel 718 ring forgings, and GTAW welded to the shell.

All flanged joints use double conical seals, except the large diameter main flange. The main flange is sealed by a narrow (.060-in.) circumferential GTAW weld.

The 26.5-in. diameter hemisphere is formed from a flat plate. The 90 degree transition elbows are formed into 180 degree half-shells, then welded together to form the elbow. Cutouts in the hemisphere are reinforced by transition rings. Flange hubs, slope gradually (15 degrees to 17 degrees) to a smooth transition with the housing wall. All forgings are ultrasonically inspected. Excess material remains on all flange surfaces to allow machining to final dimensions after welding, heat-treatment, and proof test.

After all parts are welded together, the assembly is solution-annealed and aged, which stress relieves the part and brings the material strength up to desired levels. The part is hydrostatically proof tested at 560 psig and helium leak tested at 275 psig. If proof and leak tests are satisfactory, the part is penetrant-inspected and welds are radiographically-inspected. The assembly is then machined to final dimensions.

9. Support Frame and Main Flange Clamps

The support frame extends from the outside diameter of the main flange to the pump discharge housing. The frame consists of three conical segments, with 72 degrees of arc to each segment. The segments are free to move radially to accommodate the thermal movements of the turbine main flange. The turbine inlet torus and the exhaust housing are also free to move, both radially and axially, from the main flange fixed point. The frame material is Inconel 718, which gives lightweight with high strength. It also provides the same coefficient of thermal expansion as the turbine components.

The support frame, clamps, and turbine main flange can be seen in their assembled position in Figure No. 2. The frame is made from Inconel 718 sheet stock, 0.188-in. thick, rolled into a 20 degree cone frustum. Flanges are welded to each end forming the attachment points. Figure No. 9 shows a single segment of the frame with an end view and a cross-section.

The main flange end of the frame segments are slotted axially for 6-in. and then every 2.3-in. in the tangential direction. This gives the required radial flexibility for the turbine thermal expansions. Two 1/2-in. high circumferential reinforcing ribs are welded to the conical section to give the required stiffness to the segments during handling and installation. The frame is fabricated as a complete cone frustum. It is then cut into five segments, three of which are used in each turbopump assembly. All heat treatment and finish machining is accomplished before the frame cone is cut into segments.

The clamps that mate with the frame ends are machined from a forged ring that approximates the finished shape. Material is Inconel 718, aged by heat-treating for maximum strength. Between the frame segments, two clamps, one on each side of the turbine main flange, are bolted together giving continuous support to the flanged joint.

## IV. CONCLUSIONS AND RECOMMENDATIONS

The electron-beam welding of the first-stage rotor shaft and the blades of both rotors to the discs was a satisfactory method for attaching these parts with a minimum of distortion and machining. It also lessened the rotor weight because of reduced rim thickness, as compared with mechanical attachment methods. However, very close tolerances were required on the blades and very complex tooling was needed to position the blades in preparation for the welding process. For a small development program, it would be less expensive to use simple tooling and hand-fit each blade.

The use of Inconel 718 material, which was fairly new at the time, caused some welding problems when using the gas tungsten arc welding method. The main problem was weld contamination (i.e., occlusions in the weld rod, impurities in the helium and argon gas shields, and dusty or dirty weld booths). Additional problems encountered included weld passes that were too large with improper cleaning between each pass causing weld cracking, part distortion, and weld occlusions. It was found that optimum weld joint configurations had to be developed for each component. This required that sample weld joints be made to obtain the best solution and to check out the welder as well as the equipment.

The design achieved the target weight goal of 960 lb with all static parts successfully passing proof test requirements. However, the turbine was not operated at design conditions.

The separable, seal-welded, housing joints proved feasible and joints of this type are recommended for hot gas flange applications because the seal welded joint has less weight and less thermal stress than a comparable joint with conventional seals.

## BIBLIOGRAPHY


1. Bartholf, L. W., Structural Analysis of M-1, Mod I FTPA Turbine Tie-Bolt P/N 286134, Aerojet-General Report No. SA-FTPA-164, 24 June 1965

2. Bartholf, L. W., Hiltz, J. P., and Smithers, O. L., Structural Analysis of the M-1 Fuel Turbine Rotors, Aerojet-General Report No. FTPA-102, 20 November 1964

3. Bartholf, L. W. and Smola, C. R., Structural Analysis of FTPA Turbine Rotor P/N 286109 for M-1 Application, Aerojet-General Report No. FTPA-124, 13 July 1965

4. Blakis, R., Lindley, B. K., Ritter, J. A., and Watters, W. E., Initial Test Evaluation of the M-1 Liquid Hydrogen Turbopump Including Installation, Test Procedures, and Test Results, NASA Report CR 54827, 20 July 1966

5. Frick, V., Hunt, V., Inouye, F. T., and Janser, G. R., Summary of Experience Using Inconel 718 on M-1 Engine, Aerojet-General Report No. 8800-37, 1 March 1966 (To be published as a NASA Contractor report)

6. Goudreau, G. L., Smithers, O. L., M-1 Fuel Test Manifold, Test Manifold Brace Kit, and Turbine Inlet Manifold, Aerojet-General Report No. SA-FTPA-127, 21 April 1965

7. Hiltz, J. P., Smithers, O. L., Structural Analysis of M-1 Fuel Turbine Inlet Manifold with Nozzle Assembly, Aerojet-General Report No. FTPA-SA-129, 9 March 1965

8. Radkowski, P. P., Davis, R. M., and Boldul, M. R., A Numerical Analysis of the Equations of Thin Shells of Revolution, Avco Corporation

9. Regan, P. J., Mechanical Design of the M-1 Axial Flow Hydrogen Fuel Pump, NASA Report CR 54823, 15 February 1966

10. Reynolds, T. W., Aerodynamic Design, Model II Turbine M-1 Fuel Turbopump Assembly, NASA Report CR 54820, 15 April 1966

11. Severud, L. K., Stress Analysis of the M-1, Mod II Turbine Exhaust Housing, P/N 286144, Subjected to Internal Pressure and Line Induced Loading, Aerojet-General Report No. FTPA-112, 31 December 1964

12. Severud, L. K., Stress Analysis of the M-1, Mod II Turbine Inlet Manifold - Exhaust Housing Joint, Aerojet-General Report No. FTPA-120, 31 December 1964

## BIBLIOGRAPHY (Cont'd)


13. Smithers, O. L., Structural Analysis of M-1 Fuel TPA Bearing Housing Seal Assembly P/N 286116, Aerojet-General Report No. SA-FTPA-174, 26 July 1965

14. Toms, R. M., M-1 Fuel Pump Turbine Blade Resonant Speeds, Aerojet-General Report No. FTPA-108, 2 December 1962

15. Sponseller, R. L. and Toms, R. M., M-1 Fuel Pump Turbine Blade Stress Analysis, Aerojet-General Report No. FTPA-118, 31 December 1964

16. ASME, Section III, ASME Boiler and Pressure Vessel Code for Nuclear Vessels, p. 6, Library of Congress, Catalog Card No. 56-3934, 1963